Late Silurian zircon U–Pb ages from the Ludlow and Downton bone beds, Welsh Basin, UK

Elizabeth J. Catlos[1]*, Darren F. Mark[2,3], Stephanie Suarez[1,4], Michael E. Brookfield[1,5], C. Giles Miller[6], Axel K. Schmitt[7], Vincent Gallagher[2] and Anne Kelly[2]

[1] Department of Geological Sciences, Jackson School of Geosciences, The University of Texas at Austin, Austin, TX 78712, USA
[2] Isotope Geosciences Unit, Scottish Universities Environmental Research Centre, University of Glasgow, Rankine Avenue, East Kilbride G12 8QQ, UK
[3] Department of Earth and Environmental Sciences, University of St Andrews, St Andrews KY16 9AJ, UK
[4] Present address: Department of Earth and Atmospheric Sciences, University of Houston, Houston, TX 77004, USA
[5] School for the Environment, University of Massachusetts at Boston, Boston, MA 02125, USA
[6] Department of Earth Sciences, The Natural History Museum, London SW7 5BD, UK
[7] Institut für Geowissenschaften, Ruprecht-Karls-Universität Heidelberg, 69117 Heidelberg, Germany
EJC, 0000-0001-6043-3498; CGM, 0000-0001-9111-2136
* Correspondence: ejcatlos@jsg.utexas.edu

Abstract: The Ludlow Bone Bed (Welsh Basin) is a critical stratigraphic horizon and contains a rich assemblage of fish scales. Units above provide insights into the early evolution of animal and plant life. The bed has not yet been radioisotopically dated. Here, we report 207 secondary ion mass spectrometry (SIMS) ages from 102 zircon ($ZrSiO_4$) grains from the Ludlow ($n = 2$) and stratigraphically higher Downton ($n = 1$) bone beds. SIMS ages are middle Ordovician (471.6 ± 20.7 Ma) to late Devonian (375.7 ± 14.6 Ma, $^{238}U–^{206}Pb$, $\pm 1\sigma$ analytical uncertainty). Cathodoluminescence images show that the youngest ages appear affected by alteration. Chemical abrasion isotope dilution thermal ionization mass spectrometry (CA-ID-TIMS) U–Pb geochronology was utilized to improve precision. Detrital zircon grains from Downton yield $424.91 \pm 0.34/0.42/0.63$ Ma and from Ludlow $424.85 \pm 0.32/0.41/0.62$ Ma ($n = 5$ each, $^{238}U–^{206}Pb$, $\pm 2\sigma$ analytical, tracer or systematic uncertainty). These ages provide a maximum deposition age. Results overlap the basal Přídolí age (423.0 ± 2.3 Ma) in its stratotype (Požáry Section, Reporyje, Prague, Czech Republic). The Ludlow Bone Bed marks the base of the local Downton Group, which has previously been correlated with the base of the Přídolí Series. The CA-ID-TIMS ages are older than those for other land arthropod-bearing sediments, such as the Cowie Harbour Fish Bed and Rhynie Chert.

Supplementary material: An Excel file containing detailed information on the SIMS analyses, a figure showing calibration curves for AS3 standards sputtered over sessions 1 and 2, and a figure showing CA-ID-TIMS U–Pb age data (concordia and weighted mean plots) are available at https://doi.org/10.6084/m9.figshare.c.5087031

The late Silurian was a time of change from a marine to a non-marine environment in the area of the Welsh Borderland, marking the final stages of the closure of the Iapetus Ocean, and an interesting interval for the evolution of life in general (e.g. Allen 1985; Calner 2008; Munnecke et al. 2010; Blain et al. 2016). Some of the oldest land arthropods have been discovered (Jeram et al. 1990; Shear et al. 1998) just above the level of a concentration of fish scales in a bone bed that British geologist Roderick Impey Murchison (1792–1871) first mentioned in 1834 and later called the Ludlow Bone Bed (Murchison 1853). The Ludlow Bone Bed itself is considered the type locality of several species of late Silurian fishes and was long thought to mark the first appearance of fossil fishes in the rock record (e.g. Symonds 1872; Hinde 1904; Rowlands 1988). Some of the earliest vascular land plants have been recovered from Wenlock age sediments and stratigraphic horizons just below the Ludlow Bone Bed in the Welsh Borderland (Edwards and Kenrick 2015).

Evaluating the rate and character of land colonization requires precise dating of such early land biotas. However, the age of the Ludlow Bone Bed horizon is subject to controversy. For many years, the bed was taken to represent the Silurian–Devonian boundary (see White 1950; Jones 1955; Miller 1995, for a brief history). However, ratification of the 'golden spike' for this

boundary at a higher stratigraphic level in the Barrandian Basin in the Czech Republic (Chlupác 1972) meant that a fourth series of the Silurian was needed to follow the Llandovery, Wenlock and Ludlow (Ogg et al. 2008). Bassett et al. 1982 suggested that the level could be used to define the base of a new 'Downton Series', but a level was subsequently chosen in the Barrandian Basin, Czech Republic and the fourth series was ratified as the Přídolí Series with its base coincident with the base of the *Monograptus parultimus* biozone (Bassett 1985; Kříž et al. 1986). Conodont and ostracod distributions across this level have been used in correlation to suggest that the Ludlow Bone Bed at Ludlow is the local representative of the Ludlow–Přídolí Series boundary in the Welsh Borderland (Siveter et al. 1989; Miller 1995; Märss and Miller 2004).

Conodont evidence has also been used to suggest that the base of the Přídolí Series may be higher than the Ludlow Bone Bed horizon (Schönlaub 1986; Aldridge and Schönlaub 1989). Loydell and Fryda (2011) have similarly suggested that this level is older than basal Přídolí and represents the mid-Ludfordian positive carbon isotope excursion based on an isotope analysis of a nearby section at Downton (Fig. 1), the distribution of conodonts and thelodonts and the fact that this level is represented by a significant facies change indicating shallowing. The facies change towards a non-marine environment at this level makes it difficult to correlate outside the
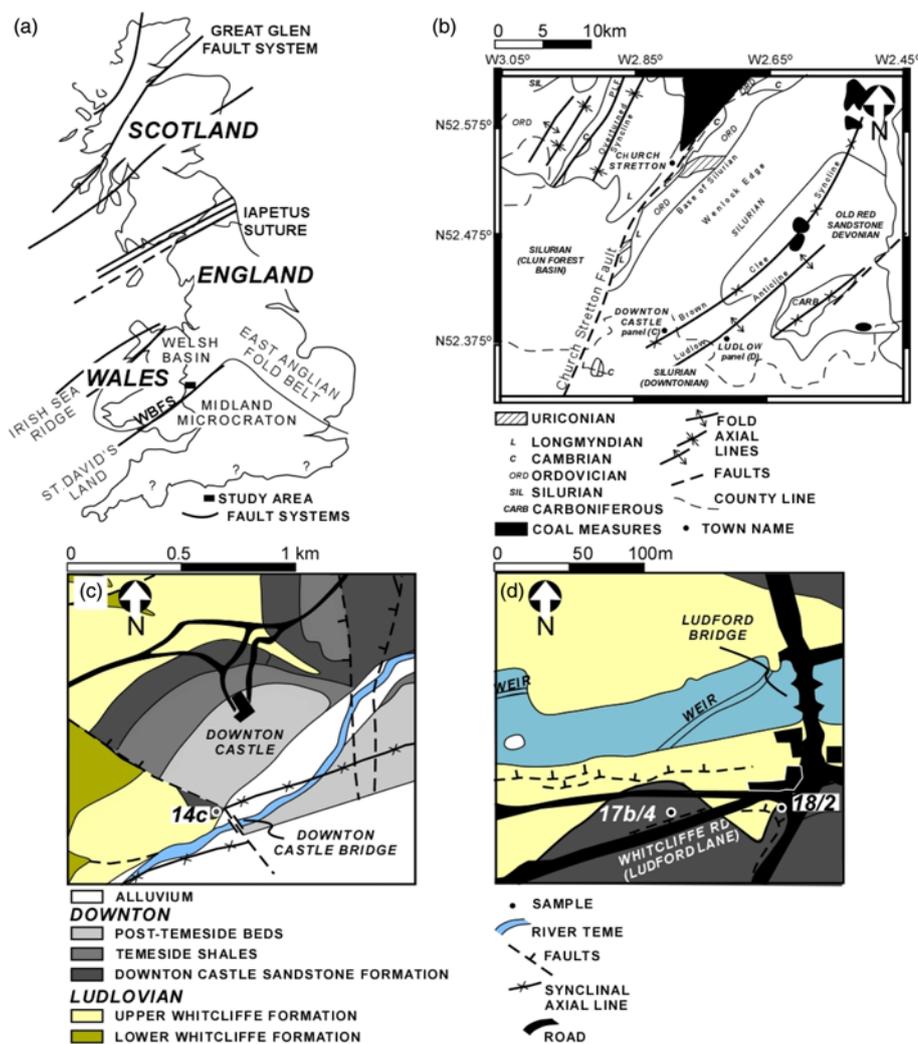
Fig. 1. (**a**) Location of samples analysed in this study. Boundaries of palaeostratigraphic components after Allen (1985), and location of significant fault systems (some labelled) after Woodcock and Gibbons (1988). WBFS, Welsh Borderland Fault System. (**b**) Geological structure map of the Shropshire area showing the context of the field area after Butler (1990). Permission provided by the Shropshire Geological Society. (**c**) Sample 14c locality near the Downton Castle Bridge. Geological map after Whitaker (1962). (**d**) Locations of samples 17b/4 in Ludford Lane and 18/2 at Ludford Corner. Geological map after British Geological Survey (1973) 1:25 000 series, Classical areas of British Geology, sheet SO47, SO57 Leintwardine Ludlow. Contains British Geological Survey materials © UKRI 1973.

Welsh Borderland as no graptolites have been reported (e.g. Ogg *et al.* 2008).

This contribution aims to use zircon U–Pb geochronology to constrain a maximum depositional age for the sediments located above the Bone Bed at Ludlow and at Downton to place the early land animal and plant biota into a temporal context, particularly following the re-dating of the Cowie Harbour Fish Bed, Aberdeenshire (Suarez *et al.* 2017). Both U–Pb secondary ion mass spectrometry (SIMS) and chemical abrasion isotope dilution thermal ionization mass spectrometry (CA-ID-TIMS) techniques were used to date zircon. The results have implications for understanding the timing of major biotic events in Earth history and establishing the stratigraphy of the latest stages of the Silurian (Brookfield *et al.* 2020).
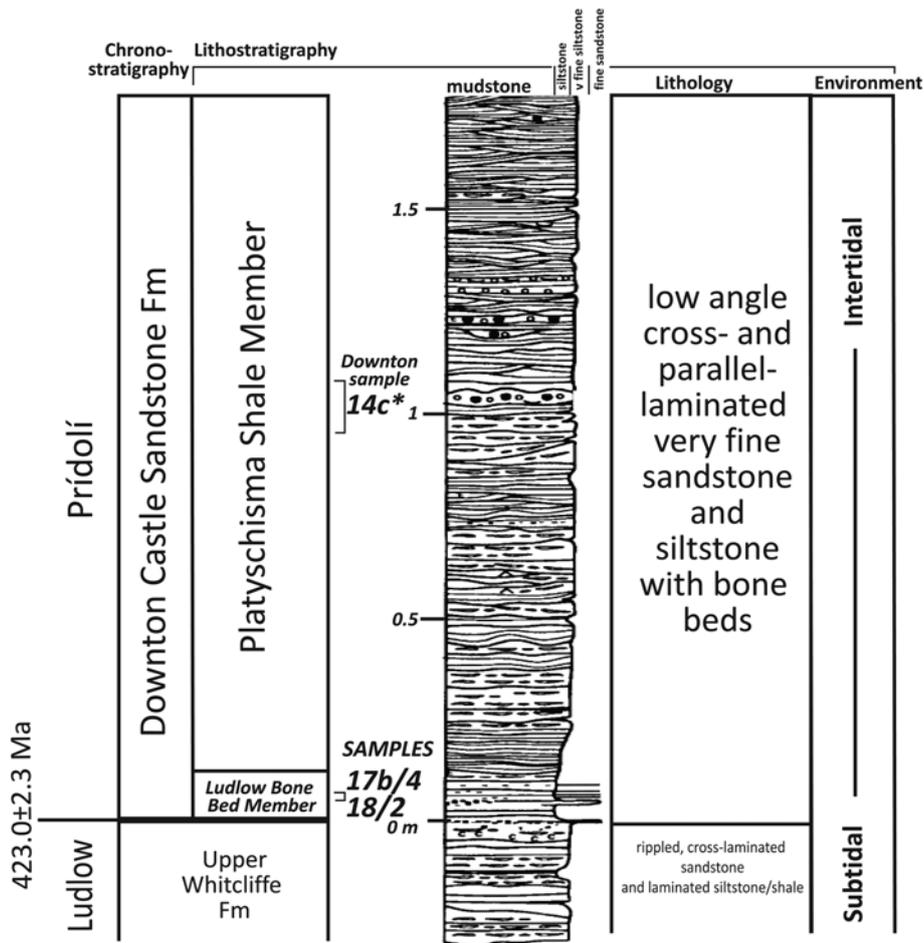
Lithostratigraphy and sedimentology

The three samples analysed are from key stratigraphic sections that are internationally recognized localities (e.g. Holland 1982; Rowlands 1988; Lawson and White 1989; Siveter *et al.* 1989; Jeram *et al.* 1990; Rogers 2017; Hauser 2019). They are positioned at the junction between the Upper Whitcliffe and Downton Castle Sandstone formations (Figs 1 and 2; e.g. Whitaker 1962; Holland *et al.* 1963; Bassett *et al.* 1982; Miller 1995). Sample 17b/4 of Miller (1995) was taken from a bone bed 10 cm above the base of the Ludlow Bone Bed Member on Ludford Lane [UK Grid reference SO 5117 7413] (Figs 2 and 3). This location is next to the speed limit sign 80 m WSW of the Ludford Corner type section for

the Ludlow Bone Bed, which is at the junction of Whitcliffe Road and the Ludlow to Leominster Road at Ludford Bridge, Ludlow. Sample 14c was taken from the Downton Bone Bed of the Platyschisma Shale Member of the Downton Castle Sandstone Formation (Miller 1995, p. 345) and was collected by Lennart Jeppsson in 1968 in a track section in a field to the south of Downton Castle Bridge [SO 4442 7402]. This stratigraphic level is no longer exposed or accessible but was interpreted as being above the Ludlow Bone Bed (Whitaker 1962). Sample 18/2 (Miller 1995) was taken from Ludford Corner at the junction of the A49 with Ludford Lane [SO 5124 7413] (Siveter *et al.* 1989, location 3.2a), and from the Ludlow Bone Bed *sensu stricto*, the lowest bone bed in the Ludlow Bone Bed Member of the Downton Castle Sandstone Member. Photographs of the exact locations of samples 18/2 and 17b/4 are shown in the paper by Bassett *et al.* (1982, text-figs 4 and 5 respectively). All samples have been previously analysed for conodonts (Miller and Aldridge 1993; Miller 1995), and 17b/4 and 18/2 are from the Teme Bank Site of Special Scientific Interest (SSSI), whereas 14c is from the River Teme SSSI. All rocks were sampled in such a way that the aesthetic qualities of rock exposures were preserved, and so that sampling did not damage or destroy their geoheritage value for future generations, and complied with ethical geological sampling policies.

The Upper Whitcliffe Formation consists of rippled and parallel laminated, very fine sandstones with alternating clay–silt laminae, containing mega-ripples, scour channels infilled with shell debris and convolute slump bedding (e.g. Allen 1985). The overlying Downton Castle Sandstone Formation at its type section in Ludlow

Fig. 2. Stratigraphy and detailed section at Ludlow showing the transition between the Upper Whitcliffe Formation and the Downton Castle Sandstone Formation (after Miller 1995). The lithology and environment columns are added based on stratigraphic interpretations (e.g. Bassett *et al.* 1982; Edwards 1996). We acknowledge copyrighted material in this figure from the Palaeontological Association; specifically, see Miller 1995 (text-fig. 6) for detailed stratigraphy of the sections located for 17b/4 and 18/2. *We infer the position of sample 14c in this figure as being in the Platyschisma Shale Member, *c.* 1 m above the base of the Ludlow Bone Bed Member. It should be noted that many discontinuous bone beds are marked in the adjacent section, and a possibility exists that it could correlate with any of these, or even a bone bed higher than this level. Timescale after Cohen *et al.* 2020.

is divided into three different members. The 0.2 m thick Ludlow Bone Bed Member is the lowest, and consists of lenticular and ripple laminated siltstones containing several discontinuous thin vertebrate-rich sands (Siveter 2000). Similar bone beds have been discovered at other locations across the Welsh Borderland (Fig. 2) and are considered to represent the lithostratigraphical boundary between the Upper Whitcliffe Formation and the Downton Castle Sandstone Formation, or their local correlatives.

The Platyschisma Shale Member of the Downton Castle Sandstone Formation is up to 2 m thick and consists of parallel and cross-laminated very fine sandstones with subordinate mudstones and siltstones (Bassett *et al.* 1982; Smith and Ainsworth 1989; Siveter 2000). The following Sandstone Member (not shown in Fig. 2) continues a coarsening upward sequence and consists of alternating sandstones and siltstones with thin, erosive based, normally graded units with sharp current- or
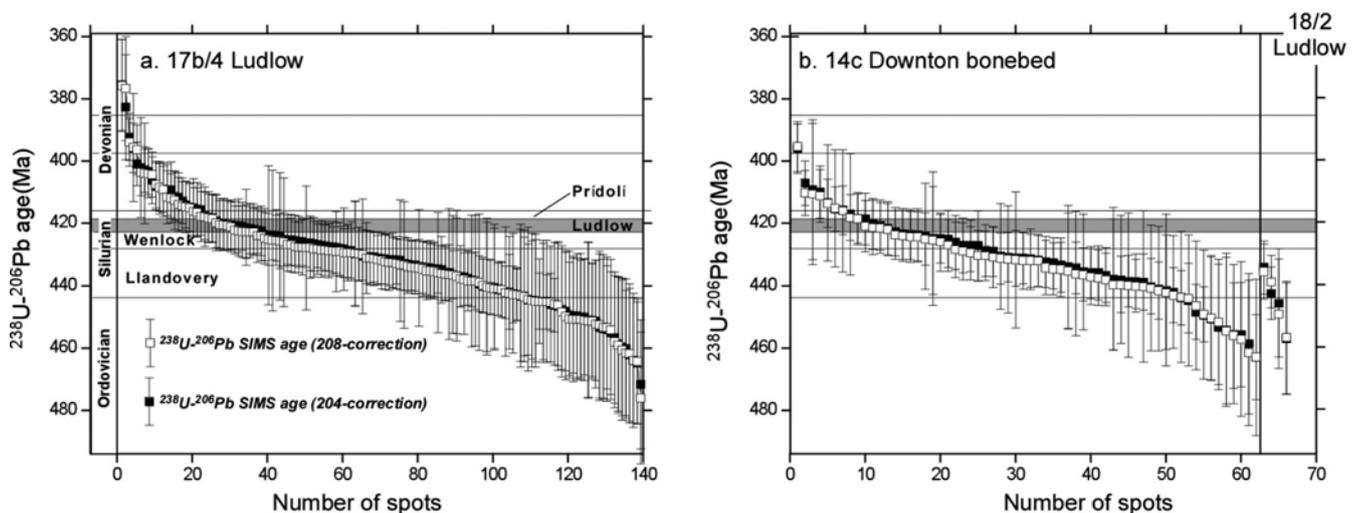
Fig. 3. Zircon age distribution for (**a**) sample 17b/4 and (**b**) samples 14c and 18/2. The plot shows the results using both common Pb corrections. Figure 4 shows the concordia diagrams for the dated grains that are discussed in the text. Timescale divisions after Ogg *et al.* 2008.

wave-rippled tops (Allen 1985). Smith and Ainsworth (1989) also recognized hummocky cross-stratification.

Palaeontology and biostratigraphy

The macro-faunal content of the beds above and below the Ludlow Bone Bed horizon at Ludlow has been summarized by Bassett *et al.* (1982, text-fig. 6), Siveter *et al.* 1989 and Siveter (2000, text-fig. 6.5). In general, a brachiopod-dominated fauna for the Upper Whitcliffe Formation has been replaced by a bivalve- and gastropod-dominated fauna with an associated change in ostracod fauna. The bone bed itself contains both marine and terrestrial fossils (e.g. Dunlop 1996). Scales in the deposits are made from dentine and have classic histology consistent with bone. Individual scales are abraded and not well preserved. The vertebrate remains have been widely studied (Agassiz 1839; Harley 1861; White 1950; Turner 1973, 2000; Antia 1980; Dineley and Metcalf 1999; Märss and Miller 2004). These consist mainly of thelodont and acanthodian dermal denticles with nonarticulate brachiopod fragments and abraded authigenic quartz crystals. Marine fauna within the Ludford Lane sequence is reported to be primarily eurypterids but also aquatic scorpions, scolecodonts, thelodont denticles and conodonts (Manning 1993; Dunlop 1996). Vascular land plants have been reported, including *Cooksonia* at Ludford Lane, and sterile rhyniophytoid axes with stomata, this being the first demonstration of stomata in the Silurian (Jeram *et al.* 1990). Fragmentary plant remains, including spores, suggest evidence of plant–animal interactions in the Silurian (Richardson and Lister 1969; Edwards 1996; Edwards and Kenrick 2015).

Animal fossils of organically preserved cuticle recovered by HF maceration have been recovered from the Ludlow Bone Bed Member and the lowermost part of the Playschisma Shale Member of the Downton Castle Sandstone Formation. Only a single reasonably intact individual, a trigonotarbid, has been found and is considered one of the earliest known non-scorpion arachnids (Dunlop 1996). Fragments of eoarthropleurids (Shear and Selden 1995), cutigeromorph centipedes (Shear *et al.* 1998), and scorpions have been identified and numbers of other specimens cannot reliably be assigned to taxa but may include spiders and archaeognath insects (Shear and Selden 1995).

Conodonts have been recovered from the uppermost Upper Whitcliffe Formation and the Ludlow Bone Bed Member (Aldridge and Smith 1985; Miller and Aldridge 1993, 1997; Miller 1995). However, they are rare, and those found in bone beds have been abraded, making them difficult to identify, and it cannot be discounted that they are reworked. The conodont *Ozarkodina* cf. *crispa* discovered just below the base of the Ludlow Bone Bed Member offers the possibility to correlate directly with the basal Přídolí stratotype where this species is confined to the Ludlow Series (Miller 1995). More recent conodont studies have suggested that this specimen is more indicative of mid-Ludlow forms (Viira and Aldridge 1998). The ostracod *Frostiella groenvalliana* first appears at the base of the Ludlow Bone Bed Member (Miller 1995) and via indirect correlation with more marine successions in the Baltic appears to be confined to the basal Přídolí (Siveter 2000, fig. 6.7 and references therein).

Palaeoenvironments

The field area is located in the Welsh Basin (Fig. 1), which experienced a transition from deep-water marine to continental, freshwater conditions owing to the closure of the Iapetus Ocean in the late Paleozoic (e.g. Allen 1985; Cave and Loydell 1998). This transition has been suggested to influence the evolving flora as the pace of change appears to have been 'unusually rapid' and non-

uniform, with the erosional environments contributing to the bone bed undergoing significant changes as well (e.g. Allen 1985). Lateral facies comparisons are, however, limited by major post-Silurian transcurrent movements on the family of NE–SW-oriented faults, such as the Great Glen, Highlands Boundary, Southern Uplands and Welsh Border Boundary faults, which separate disparate structural blocks in the British Isles and show hundreds to even thousands of left-lateral displacement (Dewey *et al.* 2015). Dewey and Strachan (2003) calculated that about 1200 km of cumulative sinistral strike-slip motion took place between Laurentia and Baltica from about 435 to 395 Ma.

The overall environment of the Upper Whitcliffe–Ludlow Bone Bed–Platyschisma Shale–Downton Castle Sandstone is analogous to a regressive shoreline environment, similar to a modern gulf lagoon–barrier complex (see Antia 1980). In this example, subtidal–intertidal facies (Upper Whitcliffe Formation) pass upwards into intertidal laminated silts (Platyschisma Shale Members) subject to storm reworking in tidal channels (Ludlow and other bone beds). The Upper Whitcliffe Formation may represent a shallow marine nearshore environment (Allen 1985), whereas the Ludlow Bone Bed has been interpreted as a nearshore lag deposit into which terrestrial plant and animal material was transported and reworked during severe storms (Antia and Whitaker 1978; Antia 1980; Smith and Ainsworth 1989; Richardson and Rasul 1990; Manning 1993; Manning and Dunlop 1995; Dunlop 1996). High amounts of Ir detected within the unit have been suggested to represent direct precipitation from seawater as opposed to a meteorite impact event (Schmitz 1992). The presence of *Cooksonia* mesofossils led Edwards (1996) to suggest that the environment may have been non-marine coastal habitats, such as stream banks. Palynomorphs from the Ludlow Bone Bed Member show marked changes in depositional environments indicating reworking (Richardson and Rasul 1990). Antia (1980) suggested a volcanic origin for some constituents. Based on a summary of reported palaeogeography data, the Ludlow infilling of the Welsh Basin is thought to represent about 8 myr of deposition (Allen 1985). The Ludford Lane deposit has a reported age of *c.* 414 Ma (uncertainty not reported, Jeram *et al.* 1990; also cited by Shear and Selden 1995).

In some parts of the Platyschisma Shale Member, plant- and animal-rich blocks of finely laminated siltstone form breccias within channels (Shear and Selden 1995). Transport of marsh facies (plant- and arthropod-bearing siltstone blocks) occurred through these tidal channels across a sand–silt ridge (Downton Castle Sandstone Formation). Palynomorphs from the Platyschisma Shale Member show a variable but strong marine influence (see table 2 of Richardson and Rasul 1990). On the other hand, the Platyschisma Shale could be the result of large tsunamis, which would explain the mixing of land-derived and offshore marine materials. This mix is typical of tsunamis and distinguishes them from normal storms as their waves penetrate much farther inland, and their backwash transports land material far offshore; in fact, sometimes into ocean currents and then across oceans (Brookfield 2004; Bourgeois 2009). Such tsunamis can be triggered by meteorite impacts into oceans, such as the end of the Cretaceous impact, whose deposits in Texas have similarities to the Platyschisma Shale, as Schmitz (1992) noted. A test of the impact hypothesis would be an analysis of the platinum group elements in the bed; meteorites have very different platinum group element ratios from those derived from terrestrial ultrabasic rocks (Brookfield *et al.* 2010).

To summarize, zircons found within the bone beds represent either material that has been transported into the basin by rivers or airfall zircons that have settled through the water column following the eruption of nearby volcanoes. However, for the purpose of this study, our approach to the dating experiments is to consider the zircon grains as detrital components of a sedimentary system. As such, there is potential for us to observe an over-dispersed age

population, and any interpretation of a zircon population age will yield a maximum depositional age for the bone beds.

Materials and methods

Several conodont residues from Miller (1995) were examined for suitable zircons, but only the three samples proved successful. These were samples 14c ($n = 23$ grains), 17b/4 ($n = 77$) and 18/2 ($n = 2$) (Fig. 1). Zircons were extracted by sonicating the residue samples in a bath of hydrogen peroxide and water. In this approach, clay minerals rise to the top of the bath, whereas zircon and other heavy minerals sink owing to density differences. The method is similar to that reported by Hoke et al. 2014. The grains are easily identified in the separates, and no chemicals commonly used for mineral extraction are needed.

Each zircon was examined optically during the mounting process to eliminate visibly cracked or metamict grains. Grains were mounted in epoxy with AS3 zircon reference (1099.1 ± 0.5 Ma; Schmitz et al. 2003) at Heidelberg University (Germany) and polished to expose their approximate cross-sections. After sectioning, each grain was imaged in cathodoluminescence (CL) using a LEO 440 scanning electron microscope (SEM) fitted with a GATAN MiniCL detector at Heidelberg University. These images were used to determine ideal locations for analysis. The mounts were cleaned in ethylenediaminetetraacetic acid (EDTA) disodium salt dehydrate ($C_{10}H_{14}N_2Na_2O_8.2H_2O$) followed by methanol and distilled water to reduce the potential for common Pb contamination (Lukács et al. 2018). Mounts were coated in gold and dated. In this approach, an oxygen beam (c. 20 µm spot size) sputters isotopes of U, Th and Pb from the surface to a depth of <5 µm on the zircon grain. Given the small amount of sample consumed, the approach is minimally destructive and allows for future analysis of these grains by the same or different methods if desired.

We report 207 SIMS ages from 102 zircon grains (Figs. 3 and 4, Supplementary material, Table S1). SIMS ages were obtained using a CAMECA IMS 1280-HR ion microprobe at Heidelberg University. Two analytical sessions were performed using the ion microprobe. In both sessions, a calibration curve was developed using U and Pb isotopic data from spot analyses of the AS3 zircon reference (Supplementary material, Fig. S1). A 10–15 nA ^{16}O primary beam was focused to a spot of 10–15 µm diameter to generate +10 kV secondary ions. The mass resolution was set to c. 7000, and oxygen flooding was applied to increase Pb$^+$ yields. Presputtering time of 30 s was set to remove potential surficial contamination. For each analysis, secondary ion intensities were acquired in nine magnet cycles through the species $^{94}Zr_2^{16}O$, ^{204}Pb, ^{206}Pb, ^{207}Pb, ^{208}Pb, ^{232}Th, ^{238}U, $^{238}U^{16}O$ and $^{238}U^{16}O_2$. Standard AS3 grains were analysed after every five to six unknown spots.

The first session occurred over a 2 day time frame, and 55 spots were placed on the AS3 zircon reference. A calibration curve of $UO_2^+/U^+ = 0.5059(Pb^+/U^+$, relative sensitivity factor$) + 0.7350 \pm 0.0256$ reproduced the ^{238}U–^{206}Pb age of AS3 to 1096 ± 47 Ma ($\pm 1\sigma$); age uncertainty is an estimate for analytical precision. The UO_2^+/U^+ values sputtered from the AS3 grains average 1.48 ± 0.02, with a range of 1.57 ± 0.30 to 1.41 ± 0.2. The second session lasted over the span of 1 day, and 26 spots were placed on AS3. The calibration curve for the second day of analysis is defined by $UO_2^+/U^+ = 0.8131(Pb^+/U^+$, relative sensitivity factor$) + 0.3561 \pm 0.0269$ and reproduced the ^{238}U–^{206}Pb age of AS3 to 1099 ± 53 Ma. The UO_2^+/U^+ values sputtered from the standard grains average 1.78 ± 0.01 and defined a larger range from 1.91 ± 0.01 to 1.68 ± 0.01. The larger UO_2^+/U^+ range during the second analytical session contributed to the smaller uncertainty observed for the unknowns.

All analyses on reference zircon AS3 were reduced using a common ^{204}Pb correction, whereas the unknown grains were subjected to both ^{204}Pb and ^{208}Pb corrections. Table S1 includes

details regarding the ages obtained using both corrections. Data reduction, concordia diagrams and age calculations were performed using the software package ZIPS (v3.1.1; C. Coath, University of Bristol). Common Pb corrections were applied using the evolution model of Stacey and Kramers (1975) and decay constants and ratios recommended by Steiger and Jäger (1977). Uncertainties of the decay constants are included in the U–Pb ages. During SIMS analysis, reflected light images were taken of each spot. We used these images to determine the location of the spot with respect to zircon grain CL zoning. It should be noted that all SIMS ages discussed in the text are ^{238}U–^{206}Pb ages and are reported with $\pm 1\sigma$ uncertainty. Zircon U/Th standard 91500 (1065 ± 0.3 Ma, U = 81.2 ppm, Th = 28.6 ppm; Wiedenbeck et al. 1995, 2004) was analysed during the second session of analysis, which allows an estimation of zircon spot U and Th contents. This standard yields a ^{238}U–^{206}Pb age of 1114 ± 21 Ma ($^{207}Pb/^{235}U$ age of 1085 ± 24 Ma, $^{207}Pb/^{206}Pb$ age of 1028 ± 57 Ma).

After SIMS U–Pb geochronology, six zircons from sample 17b/4 and five from sample 14c were selected for further dating using CA-ID-TIMS high-precision U–Pb dating at the Scottish Universities Environmental Research Centre (SUERC) at the University of Glasgow (Fig. 5). The process involved removing the individual zircon grains from the SIMS epoxy mount. For sample 17/b4 grains 47 (CA-ID-TIMS grain number 01), 43 (02), 68 (03), 70 (04) and 67 (05) were selected for dating (Fig. 6a, b, d, h and l). From sample 14c grains 13 (01), two (02), three (03), seven (04), 12 (05) and six (06) were selected for dating (Fig. 7a, e, f and g).

Zircons were dated using CA-ID-TIMS at SUERC using methods for chemical abrasion that are modified from Mattinson (2005). Zircon grains were annealed in custom-made quartz crucibles in a muffle furnace at 900°C for 60 h. Following annealing, they were leached in a solution of 29M HF and trace HNO_3 in a steel-jacketed reaction vessel at 215°C for 12 h. Prior to dissolution, zircon were rinsed multiple times in 15M HNO_3 before single grains were placed in 200 µl PFA microcapsules with c. 100 µl of 29M HF, trace HNO_3 and 6 µl of a mixed ^{205}Pb–^{235}U tracer (SUERC in-house tracer SK5a, which is consistent with the ^{205}Pb tracer described by Parrish and Krogh (1987) and calibrated against the EarthTime solutions of Condon et al. (2015). Grains were dissolved in steel-jacketed dissolution vessels at 215°C for at least 60 h. Following dissolution, the microcapsules were removed, the samples dried on a hotplate, and then c. 100 µl of 6.2M HCl were added and the microcapsules were returned to the steel-jacketed dissolution vessels at 180°C for c. 12 h. Finally, the samples were dried in the microcapsules again and taken up in c. 175 µl of 3M HCl. Uranium and Pb were separated using anion-exchange resin in 50 µl microcolumns using an HCl elution scheme modified from Krogh (1973). The U and Pb fractions were combined and dried down with dilute phosphoric acid, and finally loaded onto degassed, zone-refined Re filaments with 1–2 µl of a Si-gel prepared by modifying the SigmaAldrich-based formula described by Huyskens et al. (2012).

The new data were collected using a recently upgraded Sector-54, including a new Daly detector, 10^{12} Ohm amplifiers, cups and acquisition unit. Lead was run as a metal and measured peak hopping on the Daly photomultiplier. Uranium was analysed as UO_2 and was either measured statically on a series of Faraday cups or by peak hopping on the Daly photomultiplier. For the mass fractionation correction, repeated measurements of SRM 981 yielded a Pb alpha of $0.220 \pm 0.025\%$ per a.m.u. and $0.150 \pm 0.025\%$ per a.m.u. ($\pm 1\sigma$) for the Daly and Faraday detectors, respectively. Repeated measurements of CRM U500 yield fractionations of $0.090 \pm 0.25\%$ per a.m.u. and $0.064 \pm 0.020\%$ per a.m.u. ($\pm 1\sigma$) for the Daly and Faraday detectors, respectively. We note that these are typical fractionations and uncertainties for Pb by TIMS (e.g. Sláma et al. 2008). Lead blanks are calculated by assuming that

Table 1. *SIMS data for zircon grains that yield ages that are within the Devonian and younger*

Session\ @zircon spot number[1]	$^{238}U/^{206}Pb$ age (Ma) $(\pm 1\sigma)$[2]	$^{235}U/^{207}Pb$ age (Ma) $(\pm 1\sigma)$[3]	UO_2^+/U^+ $(\pm 1\sigma)$[4]	Th/U[5]	U (ppm)[6]	$\%^{206}Pb*$ $(\pm 1\sigma)$[7]	Conc. ellipse corr.[8]
Sample 17b/4 [UK Grid reference SO 5117 7413]							
Concordant analyses							
2\ @24[9]	402.9 (7.3)	400.7 (8.6)	1.840 (0.008)	0.199	423	99.9 (0.1)	0.77
2\ @7[9]	408.7 (8.4)	411.0 (12.1)	1.740 (0.010)	0.477	269	99.7 (0.1)	0.65
2\ @53[9]	409.4 (8.3)	413.6 (11.2)	1.710 (0.011)	0.273	261	99.9 (0.1)	0.68
2\ @61[9]	411.4 (7.7)	394.5 (14.7)	1.838 (0.013)	0.342	209	99.4 (0.2)	0.42
2\ @39[9]	415.1 (9.3)	409.7 (13.0)	1.618 (0.017)	0.247	382	99.7 (0.1)	0.49
Concordant analyses but assumed to have experienced radiogenic Pb loss							
1\ @47[9]	375.7 (14.6)	376.5 (13.8)	1.601 (0.021)	0.446 (0.008)	n.m.	99.4 (0.1)	0.86
1\ @68[9]	382.9 (16.8)	384.4 (16.3)	1.520 (0.026)	0.712 (0.008)	n.m.	99.5 (0.1)	0.91
2\ @72R2[9]	392.4 (7.6)	400.5 (14.6)	1.860 (0.009)	0.269	199	99.7 (0.2)	0.47
2\@16[10]	395.8 (17.3)	272.7 (275)	1.900 (0.010)	0.206	326	68.0 (2.5)	0.65
2\ @70[9]	395.9 (7.9)	397.6 (11.4)	1.743 (0.015)	0.209	334	99.7 (0.1)	0.64
1\ @30[10]	404.1 (16.1)	410.9 (109)	1.619 (0.017)	0.317 (0.006)	n.m.	99.6 (0.3)	0.59
2\ @67R2[9]	409.4 (9.0)	409.3 (9.8)	1.726 (0.009)	0.107	957	99.8 (0.1)	0.81
2\ @72R4[10]	414.1 (8.7)	414.5 (21.0)	1.780 (0.014)	0.295	207	99.0 (0.3)	0.51
2\ @51R1[10]	414.6 (7.8)	403.6 (17.4)	1.850 (0.009)	0.234	356	99.7 (0.1)	0.38
2\ @47C[9]	415.8 (8.2)	404.7 (22.9)	1.775 (0.010)	0.268	367	98.3 (0.4)	0.43
Discordant analyses							
2\ @30R2[9]	406.3 (7.5)	411.9 (8.6)	1.800 (0.006)	0.090	947	99.7 (0.1)	0.81
2\ @12R[10]	416.7 (7.9)	430.2 (13.2)	1.820 (0.009)	0.088	875	96.6 (0.2)	0.59
Reversely discordant analyses							
2\ @68R3[9]	412.9 (7.3)	397.3 (18.4)	1.953 (0.011)	0.164	947	97.5 (0.2)	0.42
2\ @43C[9]	401.1 (7.0)	381.7 (12.2)	1.922 (0.008)	0.262	455	100 (0.5)	0.46
2\ @68R2[9]	403.5 (7.4)	372.2 (30.0)	1.854 (0.008)	0.158	727	91.3 (0.4)	0.41
2\ @72R3[9]	414.2 (7.5)	392.3 (15.5)	1.903 (0.014)	0.308	202	99.5 (0.2)	0.46
2\ @68C[9]	409.2 (7.4)	406.2 (7.5)	1.860 (0.010)	0.147	1107	99.9 (0.1)	0.82
2\ @1[9]	408.3 (7.6)	395.4 (13.2)	1.850 (0.011)	0.445	357	99.2 (0.2)	0.50
Sample 14c [UK Grid reference SO 4442 7402]							
Concordant analyses							
2\ @20R1[9]	407.2 (7.2)	400.1 (15.1)	1.937 (0.007)	0.130	391	99.1 (0.2)	0.43
2\ @3R1[10]	411.3 (8.4)	405.8 (24.7)	1.810 (0.17)	0.335	157	99.2 (0.4)	0.40
2\ @7A[9]	415.5 (7.1)	421.9 (11.1)	1.904 (0.008)	0.232	565	99.4 (0.1)	0.61
Concordant analyses but assumed to have experienced radiogenic Pb loss							
1\ @7[9]	409.3 (22.4)	393.4 (39.8)	1.480 (0.031)	0.404 (0.006)	n.m.	96.7 (0.5)	0.33
2\ @13[10]	413.7 (7.8)	426.7 (19.3)	1.780 (0.006)	0.088	712	94.6 (0.3)	0.48
1\ @12[9]	413.5 (18.7)	404.3 (29.0)	1.509 (0.026)	0.338 (0.011)	n.m.	96.9 (0.3)	0.66
Reversely discordant analyses							
2\ @12R2[9]	396.2 (7.9)	387.5 (11.8)	1.772 (0.017)	0.232	302	99.7 (0.1)	0.60

[1]The abbreviation is session calibration used (1) or (2)\ @ zircon spot number. (See Supplementary material Fig. S1 for the calibration curves used for these days.) Figure 4 shows the concordia diagrams for these data, and Figures 4 and 5 show the locations of each age on the zircon grains.
[2]Calculated ^{238}U–^{206}Pb age $(\pm 1\sigma)$.
[3]Calculated ^{235}U–^{207}Pb age $(\pm 1\sigma)$.
[4]Ratio measured in sample.
[5]Ratio based on analysis of zircon standard 91500 (Wiedenbeck *et al.* 1995; U = 81.2 ppm and Th = 29.9 ppm). This zircon was not analysed in the first session, therefore measured ion ratio $(\pm 1\sigma)$ from sample is reported for those analyses.
[6]Zircon U content in ppm calculated using zircon standard 91500.
[7]Per cent radiogenic ^{206}Pb.
[8]Concordia error ellipse correlations.
[9]Age generated using the ^{204}Pb common Pb correction, assuming $^{206}Pb/^{204}Pb = 18$, $^{207}Pb/^{204}Pb = 15.59$ and $^{208}Pb/^{204}Pb = 37.80$ (Stacey and Kramers 1975).
[10]Age generated using the ^{208}Pb common Pb correction, assuming $^{206}Pb/^{204}Pb = 18$, $^{207}Pb/^{204}Pb = 15.59$ and $^{208}Pb/^{204}Pb = 37.80$ (Stacey and Kramers 1975).
n.m., not measured.

all ^{204}Pb is derived from laboratory contamination. Total procedural blanks measured with this composition yield isotopic compositions of $^{206}Pb/^{204}Pb = 18.37 \pm 0.30$, $^{207}Pb/^{204}Pb = 15.55 \pm 0.16$ and $^{208}Pb/^{204}Pb = 38.17 \pm 0.37$ $(\pm 1\sigma)$, suggesting that it is well calibrated.

The correction for initial secular disequilibrium in the ^{238}U–^{206}Pb system owing to the exclusion of Th during zircon crystallization was implemented for each analysis using a ratio of zircon/melt

partition coefficients (f_{ThU}) of 0.33 (Rubatto and Hermann 2007), which is applicable for melts that are andesitic–dacitic in composition. It should be noted that as we do not know the source of the zircon crystals in this study, the f_{ThU} remains a source of uncertainty, and, as such, uncertainty of ± 1 (2σ) was applied, which covers the Th/U observed in most igneous rocks. In addition, we also calculated the ^{238}U–^{206}Pb ages using the Th/U in volcanic rocks from rifts and hotspots (Keller *et al.* 2015; Th/U$_{magma}$ 3.6 ±

1.0, ±2σ) to demonstrate the impact of the Th/U correction to our data (Supplementary material, Fig. S2). The change in grain ages and weighted mean ^{238}U–^{206}Pb ages is negligible, but we prefer to use the partition coefficient approach because this allows for sourcing from various magma batches and volcanoes, as well as changes in magma evolution.

All data reduction was made with the Tripoli and ET_Redux software packages (Bowring *et al.* 2011) using the algorithms presented by McLean *et al.* (2011). The U decay constants are from Jaffey *et al.* (1971). CA-ID-TIMS age data are presented as 2σ in the format ± *X*/*Y*/*Z*, where *X* represents the analytical uncertainty only, *Y* includes the uncertainty in the composition of the SK5a isotopic tracer and *Z* includes all systematic uncertainties including those that arise from the decay constants (Schoene *et al.* 2006).

Results and discussion

SIMS zircon analysis

Figure 3 reports a summary of the SIMS age data for each sample, applying both common ^{204}Pb and ^{208}Pb corrections. Four SIMS spot ages from only two grains were extracted from sample 18/2. Using only four ages to characterize the depositional history of a unit is impossible, and we report these ages only because there are no radioisotopic results from the Ludlow Bone Bed *sensu stricto*. However, more zircon grains were found in the other samples, and their SIMS ages range from 471.6 ± 20.7 to 375.7 ± 14.6 Ma in sample 17b/4 and from 464.1 ± 25.2 to 396.2 ± 7.9 Ma in sample 14c (^{238}U–^{206}Pb ages, ±1σ; Figs 3 and 4). As Figure 3 demonstrates, the ^{208}Pb-corrected ages shift some results slightly older, but errors are mostly unaffected. The correction did affect the degree of concordance of some results. Thus we examined each age to determine the most concordant. Figure 4 plots the SIMS ages from the samples using the common Pb correction that produced the results that intersected concordia. Owing to the age uncertainty, some results that appear concordant may be discordant. The majority of the analyses yield Th/U >0.1, and we found no correlation between Th/U or U (ppm) or age.

Devonian zircons (<416 Ma)

Despite the high-resolution CA-ID-TIMS ages (discussed below), a question may remain regarding the significance of the youngest concordant dated grains in the samples obtained via SIMS. In this section, we focus on the zircon population that yield results younger than 416 Ma, considered the base of the Devonian (Table 1; Ogg *et al.* 2008). Sample 17b/4 yields 19 grains (*n* = 21 ages) that yield Devonian ages, whereas sample 14c contains six of these age zircons (*n* = 7 ages) (Table 1, Figs 3 and 4). Some SIMS ages, including the younger ones reported in this paper, may be influenced by zircon partial dissolution, metamictization or mechanical breakage. These problems are removed during the chemical abrasion of the grains before CA-ID-TIMS geochronology (e.g. Hanchar and Miller 1993; Rubatto and Gebauer 2000).

To interrogate the younger SIMS age population, we examined the CL images, per cent radiogenic ^{206}Pb* and Th/U values of each spot. We evaluated the age with respect to concordia and common Pb corrections (Figs 6 and 7). Zircon CL zoning is controlled mainly by its Dy^{3+} distribution (e.g. Mariano 1989; Remond *et al.* 1992), although other elements and structural defects may also be factors (see Hanchar and Miller 1993; Rubatto and Gebauer 2000).

Most of the SIMS Devonian-age grains are concordant (*n* = 15/22 analyses in sample 17b/4 and *n* = 6/7 analyses in sample 14c) (Fig. 4, Table 1). Discordant and reversely discordant ages are not considered. Grains with Th/U values <0.1 that appear affected by metamorphism or recrystallization in CL were also not considered.

Of the concordant ages, we indicate that 10 of the concordant results in sample 17b/4 and three of the concordant results in sample 14c may have experienced Pb loss. This estimation is based on their lower per cent radiogenic Pb, the location of the SIMS spots on darker zones in CL that appear affected by alteration, and distribution of multiple ages on single grains that are inconsistent with a core to rim growth.

For example, four zircons in sample 17b/4 have distinctly dark cores or regions near their centres (grains 47, 68, 43 and 67; Fig. 6a, b, h and l) and ages from these regions yield the youngest results for all of the spots on these grains. The distribution is inconsistent with zircon mineral growth from the core to rim. Although a lack of CL brightness is not an indicator of radiation damage, we speculate that these ages are probably from metamict zones and may have experienced Pb loss, as older ages are found on the rims of these zircons. This process affected several of the zircons in sample 17b/4, including the zircon that yields the youngest Devonian result (grain 47, 375.7 ± 14.6 Ma, Fig. 6a) and others (grain 43, 401.1 ± 7.0 Ma, Fig. 6h; grain 67, 409.4 ± 9.0 Ma, Fig. 6l). Grain 68 in sample 17b/4 has a broad and distinct dark CL core, and several spots placed on this region yield younger ages (from 382.9 ± 16.8 Ma to 412.9 ± 7.3 Ma) compared with the analysis that overlaps its rim region (433.5 ± 8.1 Ma) (Fig. 6b).

We see the same trend of recrystallized or younger cores regardless of CL brightness. For example, zircon 72 in sample 17b/4 has several ages overlapping bright regions in the core that are younger than its rim (Fig. 6e). A spot on grain 70 that yields the youngest age in sample 17b/4 overlaps a bright domain that may have been a recrystallized lamella (Fig. 6d). In sample 14c, grain 7 has a darker centre and yields 409.3 ± 22.5 Ma, with two spots on a rim that have absolute ages that are older (436.4 ± 8.4 and 430.9 ± 7.8 Ma), although these results overlap within uncertainty (Fig. 7a).

We also evaluated whether ages from the same concentric CL brightness zone on the grain yield the same age within uncertainty. Two spots on the outer rim of grain 20 in sample 14c yield ages of 443.6 ± 20.9 and 449.1 ± 8.8 Ma, but a third is younger at 407.2 ± 7.2 Ma (Fig. 7d). This grain has patchy recrystallized zones in CL. Several spots were placed on the central core section and overlapping the same brightness region in grain 3 of this sample, but ages range from 411.3 ± 8.4 to 439.6 ± 20.9 Ma (Fig. 7e).

We conducted duplicate analyses on complexly zoned zircon 7 and 12 in sample 14c to evaluate the reproducibility (Fig. 7a and b). The spot on grain 7 (sample 14c, Fig. 7a) yields concordant ages that are 430.9 ± 7.8 and 415.5 ± 8.1 Ma. This zircon has a CL texture consistent with metamorphic zoning, and the analysis intersected an inclusion, which probably influenced this result. Grain 12 has fine-scale oscillatory zoning that is truncated by patchy recrystallized zones. Both of the ages from that spot were reversely discordant, regardless of common Pb correction (Fig. 7b).

The process of evaluation with respect to concordia leaves us with five concordant Devonian zircon ages from sample 17b/4 (from 402.9 ± 7.3 to 415.1 ± 9.3 Ma) and three in sample 14c (from 407.2 ± 7.2 to 415.5 ± 7.1 Ma). In sample 17b/4, the youngest age overlaps a patchy, dark grey rim overgrowth in grain 24 (Fig. 6g). Grain 30 in this sample shows similar CL zoning, with a bright core surrounded by a darker CL rim (Fig. 6m). A spot on this zircon yields a similar age of 404.1 ± 16.1 Ma, but the large error bar makes the age challenging to interpret. We note that an adjacent spot that is similar to this age (406.3 ± 7.5 Ma) is discordant, and thus at least this zone of the zircon experienced Pb loss. The spots on grains 7 (408.7 ± 8.4 Ma; Fig. 6f) and 61 (412.1 ± 7.9 Ma; Fig. 6c) also overlap portions of mottled grey zoning, which we interpret to be a metamorphic rim overgrowth because it truncates the oscillatory-zoned parts of these zircons. Grain 39 in sample 17b/4 (415.1 ± 9.3 Ma; Fig. 6i) is metamorphic based on its mottled CL zoning and yields the oldest age within this group. It should be noted that in
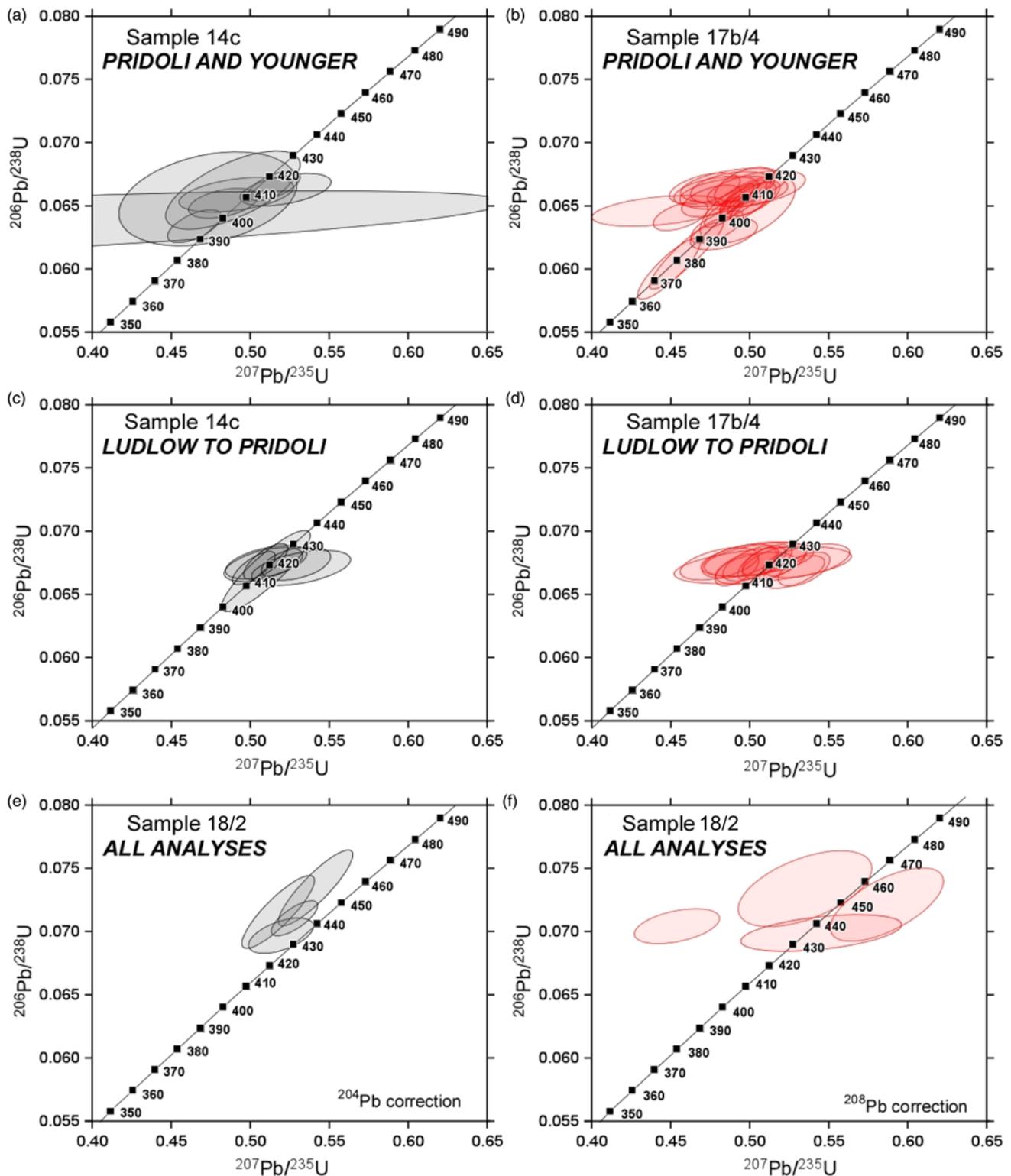
Fig. 4. Concordia diagrams for zircons dated using SIMS from (**a**) 14c, Přídolí and younger ages, (**b**) 17b/4 Přídolí and younger ages, (**c**) 14c, Ludlow to Přídolí ages (**d**) 17b/4, Ludlow to Přídolí ages, and (**e**) 18/2, all results, using the ^{204}Pb correction; (**f**) 18/2, all results, using the ^{208}Pb correction.

sample 14c, a zircon with metamorphic CL zoning has a similar age (415.5 ± 7.1 Ma; Fig. 7c).

All of the concordant ages that were interpreted as reliable from sample 17b/4 average 409.5 ± 8.2 Ma ($n = 5$, ±1σ analytical uncertainties only; weighted mean age 409.0 ± 13.2 Ma). Likewise, in sample 14c, the concordant Devonian-age zircon ages average 411.3 ± 7.6 Ma ($n = 3$, weighted mean age of 411.4 ± 18.8 Ma). Both ages are consistent with a single population, with mean square weighted deviation (MSWD) values considerably less than unity (0.3

and 0.2, respectively). The number of ages that are included in the average calculations is small, and the low MSWD values suggest that the uncertainties may be overestimated (e.g. Wendt and Carl 1991).

Ludlow–Přídolí zircons (422.9–416 Ma)

In both samples 17b/4 and 14c, several zircons yield SIMS ages within the Ludlow to Přídolí range ($n = 15$ and $n = 6$, respectively). The grains are not immune to the issues we observed with the

Table 2. *SIMS data for zircon grains that yield absolute values of ages that are within the Ludlow–Přídolí range**

Session\ @zircon spot number	^{238}U/^{206}Pb age (Ma) (±1σ)	^{235}U/^{207}Pb age (Ma) (±1σ)	UO$_2^+$/U$^+$ (±1σ)	Th/U	U (ppm)	%^{206}Pb* (±1σ)	Conc. ellipse corr.
Sample 17b/4 [UK Grid reference SO 5117 7413]							
Concordant analyses							
2\ @13†	420.0 (8.9)	417.3 (37.9)	1.680 (0.006)	0.483	224	99.2 (0.6)	0.47
2\ @26‡	421.0 (7.7)	422.0 (13.4)	1.812 (0.010)	0.124	1005	97.6 (0.2)	0.55
2\ @72R1†	421.3 (8.0)	418.4 (17.4)	1.870 (0.011)	0.194	383	99.9 (0.3)	0.50
2\ @74‡	422.3 (7.5)	419.2 (10.6)	1.915 (0.010)	0.179	357	99.8 (0.4)	0.59
2\ @47R1†	422.6 (8.0)	415.7 (23.4)	1.780 (0.006)	0.239	295	99.5 (0.4)	0.46
2\ @62†	422.8 (8.3)	413.5 (22.7)	1.820 (0.013)	0.398	156	99.8 (0.4)	0.44
Discordant analyses							
2\@12R†	416.7 (7.9)	430.2 (13.2)	1.820 (0.009)	0.088	875	96.6 (0.2)	0.59
2\ @30R1‡	418.4 (7.7)	413.7 (9.2)	1.856 (0.010)	0.163	428	99.7 (0.2)	0.66
2\ @28‡	422.0 (8.1)	435.7 (18.1)	1.837 (0.010)	0.272	287	98.8 (0.3)	0.49
Reversely discordant analyses							
2\ @38‡	417.7 (7.7)	406.2 (9.4)	1.937 (0.025)	0.409	359	99.7 (0.1)	0.58
2\ @64R1‡	418.1 (8.1)	434.7 (10.8)	1.824 (0.013)	0.273	245	100.0 (0.1)	0.55
2\ @50‡	420.6 (7.8)	398.6 (17.0)	1.870 (0.008)	0.141	460	98.2 (0.3)	0.49
2\ @11C‡	420.8 (7.8)	415.3 (8.7)	1.800 (0.010)	0.378	400	99.9 (0.1)	0.68
2\ @63‡	420.9 (8.6)	413.6 (13.4)	1.849 (0.017)	0.225	193	99.7 (0.2)	0.58
2\ @48‡	421.8 (8.1)	407.2 (16.1)	1.810 (0.012)	0.504	204	99.6 (0.2)	0.46
Sample 14c [UK Grid reference SO 4442 7402]							
Concordant analyses							
1\ @10‡	417.1 (19.4)	418.4 (18.8)	1.532 (0.026)	0.381 (0.005)	n.m.	99.7 (0.1)	0.88
2\ @22AC2‡	420.3 (8.1)	417.3 (16.8)	1.827 (0.013)	0.285	271	99.5 (0.2)	0.53
2\ @22AC1‡	420.7 (8.0)	431.1 (14.5)	1.940 (0.009)	0.289	255	99.6 (0.2)	0.40
2\ @2†	421.4 (8.7)	414.1 (24.4)	1.720 (0.007)	0.158	412	99.8 (0.4)	0.44
Concordant analyses but assumed to have experienced radiogenic Pb loss							
2\ @16R2‡	418.5 (7.9)	413.2 (9.2)	1.771 (0.006)	0.149	700	99.8 (0.1)	0.74
Reversely discordant analyses							
2\ @7R1†	418.6 (8.4)	433.3 (20.8)	1.850 (0.012)	0.504	234	98.9 (0.3)	0.47

*Row headings are as for Table 1.

†Age generated using the ^{208}Pb common Pb correction, assuming ^{206}Pb/^{204}Pb = 18, ^{207}Pb/^{204}Pb = 15.59 and ^{208}Pb/^{204}Pb = 37.80 (Stacey and Kramers 1975).

‡Age generated using the ^{204}Pb common Pb correction, assuming ^{206}Pb/^{204}Pb = 18, ^{207}Pb/^{204}Pb = 15.59 and ^{208}Pb/^{204}Pb = 37.80 (Stacey and Kramers 1975).

younger Devonian-age zircons discussed in the previous section. In sample 17b/4, nine ages yield discordant or reversely discordant results, whereas four spots dated on zircons in sample 14c are concordant (Table 2).

In sample 17b/4, the majority of the Ludlow to Přídolí-age zircon grains we examined show oscillatory zoning, consistent with a magmatic origin, although one has very low CL brightness (grain 26, Fig. 8j), and two have distinct and broad darker CL zircon cores (grains 38 and 63; Fig. 8a and b). Several are smaller, fragmented pieces with fine-grained oscillatory zoning. The youngest, concordant SIMS zircon ages in this sample in the Ludlow–Přídolí time frame are 420.0 ± 8.9 Ma, located on a bright mid-rim area on the zircon (grain 13, Fig. 8c), and 421.0 ± 7.7 Ma, located on a zircon rim (grain 26, Fig. 6j). A second spot located in the core of this grain is older (442.5 ± 19.1 Ma). All other concordant zircon ages from these samples are from spots located on zircon rims (Figs 6a, e and 8d, h). If we average these concordant results from sample 17b/4, we obtain 421.7 ± 8.1 Ma (weighted mean age, 421.7 ± 10.8 Ma). The youngest grain in sample 17b/4 is 420.0 ± 8.9 Ma (grain 13; Fig. 8c). Several other Ludlow–Přídolí zircon grains in this rock overlap this result (Table 2).

In sample 14c, the youngest concordant age considered in the Ludlow–Přídolí age range is highly uncertain (417.1 ± 19.4 Ma, Fig. 9a), whereas the second youngest is located on a darker core region that has an older rim (418.5 ± 7.9 Ma, Fig. 8c). However, grain 22A has two spot analyses that overlap in age (420.3 ± 8.1 Ma,

420.7 ± 8.0 Ma, Fig. 9b). The average of the three concordant zircon ages in sample 14c is 419.9 ± 12.1 Ma (weighted mean age of 420.5 ± 21.4 Ma).

Timescale research requires ages to be interrogated at the 2σ (95%) levels including all sources of systematic uncertainty to allow for inter-chronometer comparisons. At the 2σ confidence interval, the weighted mean SIMS U–Pb maximum depositional ages for samples 17b/4 and 14c are 421.7 ± 10.8 Ma and 420.5 ± 21.4 Ma, respectively (analytical uncertainty only). The relatively poor precision associated with these ages precludes a useful interpretation of our data with respect to the Geological Time Scale and the evolution of the Silurian fauna. Relative to the large reported uncertainties decay, constant uncertainty is negligible. As such, CA-ID-TIMS U–Pb geochronology was performed on a subset of zircon grains.

CA-ID-TIMS zircon analyses

Figure 5 and Tables 3–6 show the CA-ID-TIMS ages for zircons dated from samples 17b/4 and 14c. The weighted mean ^{238}U–^{206}Pb (Th-corrected) age for five zircons in sample 17b/4 is 424.91 ± 0.34/0.42/0.63 Ma (2σ), and for four zircons from 14c is 424.85 ± 0.32/0.41/0.62 Ma (2σ). A single older analysis (zircon 06) was rejected from age calculations from sample 14c on the basis that it is older than the young population of crystals (431.94 ± 7.5 Ma, Table 5). This grain also yields an older SIMS age (428.0 ± 8.2 Ma, Fig. 7).
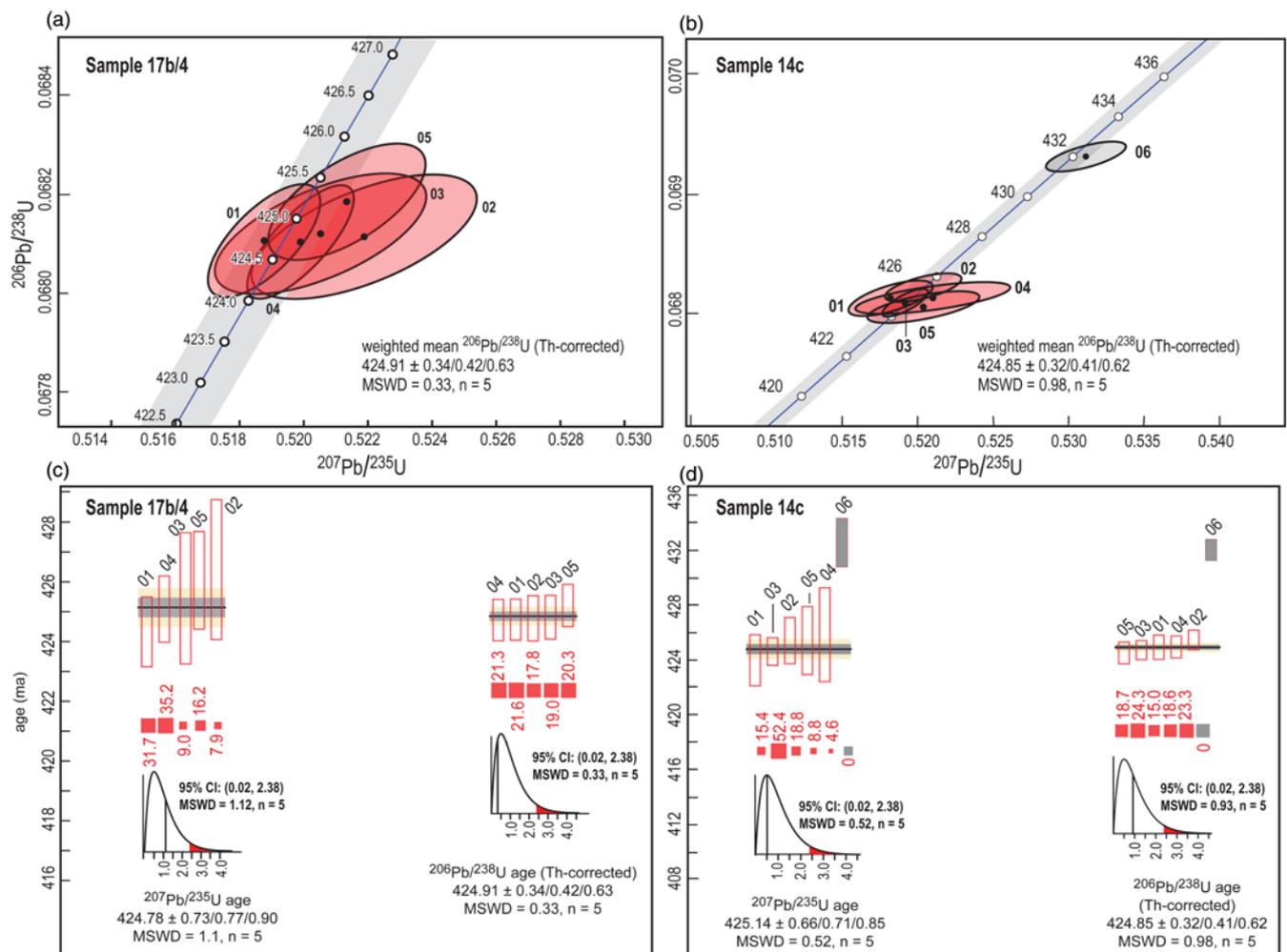
Fig. 5. Concordia diagrams for zircon grains dated using CA-ID-TIMS from (**a**) sample 17b/4 and (**b**) sample 14c. In (**c**) and (**d**), hollow bars show the ^{235}U–^{207}Pb, ^{238}U–^{206}Pb (if available) and ^{238}U–^{206}Pb (Th corrected) ages for each grain, with the length of the bar indicating the uncertainty for samples 17b/4 and 14c. CA-ID-TIMS U–Pb age data (concordia and weighted mean plots) calculated using constant U/Th$_{(magma)}$ 3.6 ± 1. The horizontal bar that runs through the hollow bars is the weighted mean average with lighter shading indicating confidence intervals. In sample 14c (**d**), we did not include grain 6 in the calculations. In (**c**) and (**d**), the red bars are the degree of weight given used in the statistical calculations, and the inset graphs are the 95% confidence intervals for the ^{235}U–^{207}Pb, ^{238}U–^{206}Pb and ^{238}U–^{206}Pb (Th corrected) ages. The summary of each of these age groups, including errors estimated using different statistical approaches, MSWD and the number of grains, is provided beneath the confidence intervals. CA-ID-TIMS age data are presented as 2σ in the format ± X/Y/Z, where X represents the analytical uncertainty only, Y includes the uncertainty in the composition of the SK5a isotopic tracer and Z includes all systematic uncertainties including those that arise from the decay constants (Schoene *et al*. 2006).

The weighted mean ages define single populations of crystals at the level of precision attainable and given population size have appropriate MSWDs (Wendt and Carl 1991). The ^{238}U–^{206}Pb ages are indistinguishable from their weighted mean ^{235}U–^{207}Pb ages (Fig. 5).

The CA-ID-TIMS ages for samples 17b/4 and 14c provide just over 1‰ precision at 2σ (*c.* ± 0.5 Ma), including decay constant uncertainty (Fig. 5). The CA-ID-TIMS ages are also indistinguishable from our weighted mean interpreted maximum deposition SIMS ages (421.7 ± 10.8 and 420.5 ± 21.4 Ma). However, the significance of these ages needs to be considered with regard to the depositional paleoenvironments. Given that we may be probably dating detrital grains, as discussed above, the level of intra- and inter-sample reproducibility is surprising.

Table 3. *CA-ID-TIMS age data for zircon grains from sample 17b/4*

Fraction*	^{206}Pb/^{238}U age (±2σ abs.)†	^{207}Pb/^{235}U age (±2σ abs.)†	^{207}Pb/^{206}Pb age (±2σ abs.)†	Conc. ellipse correlation	% discordance‡
01 (47)	424.66 (0.69)	424.3 (1.2)	422.5 (5.7)	0.688	−0.51
02 (43)	424.71 (0.76)	426.4 (2.3)	436 (13)	0.613	2.50
03 (68)	424.75 (0.73)	425.5 (2.2)	430 (12)	0.617	1.13
04 (70)	424.66 (0.69)	425.1 (1.1)	427.4 (4.9)	0.765	0.63
05 (67)	425.12 (0.71)	426.0 (1.6)	431.1 (8.5)	0.641	1.38

*Fraction is the CA-ID-TIMS grain number (SIMS grain number). (See Fig. 6a, b, d, h and l for images of these zircons.)
†Isotopic dates calculated using decay constants (λ) for $^{238}U = 1.55125 \times 10^{-10}$ and $^{235}U = 9.8485 \times 10^{-10}$ (Jaffey *et al*. 1971).
‡Per cent discordance = $100 - (100(^{206}Pb/^{238}U$ date)/$(^{207}Pb/^{206}Pb$ date)).

Implications and conclusions

Depositional age assessment

The U–Pb age of a zircon crystal from a sediment pile is clearly not related to the depositional age of the sediment. Such data can only indicate a maximum deposition age on the basis that the detrital components of sediment formed before its deposition (e.g. Condon and Bowring 2011; Gehrels 2012; Corfu 2013; Schaltegger et al. 2015; Horstwood et al. 2016; Spencer et al. 2016). The SIMS U–Pb age distribution (Fig. 3) is complicated. Some components of it will be typical of volcanic ashes in which the explosive eruptions

incorporate material from older lavas and ashes in the volcano (e.g. Guillong et al. 2014). The age profile is also defined by Pb loss, as discussed above, and potentially the analysis of grains with old zircon cores and crystals that record pre-eruptive magmatism. It should be noted that the weighted mean of all of the SIMS zircon ages we obtain in this paper from all of the samples is 426.8 ± 1 Ma (MSWD = 1.72, ±2σ). As the SIMS approach to determining U–Pb ages does not utilize chemical abrasion techniques to remove areas of Pb loss from the zircon crystals, it is difficult to use the youngest grain or analysis to infer a maximum deposition age. Pb loss could result in a zircon age that is younger than the age of deposition.

Table 4. *CA-ID-TIMS composition and isotopic ratio data for zircon grains from sample 17b/4*

Fraction[1]	Compositional data					Isotopic ratio data			
	Th/U[2]	Pb*(pg)[3]	Pbc (pg)[4]	Pb*/Pbc[5]	Th/U (magma)[6]	^{206}Pb/^{204}Pb[7]	^{206}Pb/^{238}U (±2σ %)[8]	^{207}Pb/^{235}U (±2σ %)[8]	^{207}Pb/^{206}Pb (±2σ %)[8]
01 (47)	1.48	43.7	0.98	44.792930	4.485	2178	0.06809 (0.17)	0.5188 (0.34)	0.05528 (0.25)
02 (43)	0.97	23.1	1.37	16.888336	2.939	929	0.06810 (0.18)	0.5219 (0.67)	0.05560 (0.58)
03 (68)	1.03	18.8	1.02	18.397135	3.121	998	0.06811 (0.18)	0.5205 (0.63)	0.05545 (0.54)
04 (70)	0.95	30.9	0.66	46.875019	1.909	2560	0.06809 (0.17)	0.5199 (0.32)	0.05540 (0.22)
05 (67)	0.88	24.0	0.95	25.323563	4.182	1413	0.06817 (0.17)	0.5213 (0.47)	0.05549 (0.38)

[1]Fraction is the CA-ID-TIMS grain number (SIMS grain number). (See Fig. 6a, b, d, h and l for images of these zircons.)
[2]Thorium contents calculated from radiogenic ^{208}Pb and ^{230}Th-corrected ^{206}Pb/^{238}U date of the sample, assuming concordance between U–Pb Th–Pb systems.
[3]Total mass of radiogenic Pb.
[4]Total mass of common Pb.
[5]Ratio of radiogenic Pb (including ^{208}Pb) to common Pb.
[6]Th/U ratio of magma from which mineral crystallized.
[7]Measured ratio corrected for fractionation and spike contribution only.
[8]Measured ratios corrected for fractionation, tracer and blank. Uncertainty reported at the ±2σ level in per cent.

Table 5. *CA-ID-TIMS age data for zircon grains from sample 14c*

Fraction*	^{206}Pb/^{238}U age (±2σ abs.)†	^{207}Pb/^{235}U age (±2σ abs.)†	^{207}Pb/^{206}Pb age (±2σ abs.)†	Conc. ellipse correlation	% discordance‡
01 (13)	424.84 (0.89)	424.0 (1.9)	419.2 (9.6)	0.662	−1.36
02 (2)	425.38 (0.71)	425.4 (1.7)	425.5 (8.9)	0.630	0.03
03 (3)	424.62 (0.70)	424.6 (1.0)	424.5 (4.3)	0.776	−0.03
04 (7)	424.86 (0.80)	425.8 (3.4)	431 (19)	0.662	1.44
05 (12)	424.40 (0.80)	425.4 (2.5)	431 (14)	0.641	1.50
06 (6)	431.94 (0.75)	432.6 (1.8)	435.9 (8.9)	0.669	0.92

*Fraction is the CA-ID-TIMS grain number (SIMS grain number). (See Fig. 7a, e, f and g for images of these zircons.)
†Isotopic dates calculated using decay constants (λ) for ^{238}U = 1.55125 × 10$^{−10}$ and ^{235}U = 9.8485 × 10$^{−10}$ (Jaffey et al. 1971).
‡Per cent discordance = 100 − (100(^{206}Pb/^{238}U date)/(^{207}Pb/^{206}Pb date)).

Table 6. *CA-ID-TIMS composition and isotopic ratio data for zircon grains from sample 14c*

Fraction[1]	Compositional data					Isotopic ratio data			
	Th/U[2]	Pb*(pg)[3]	Pbc (pg)[4]	Pb*/Pbc[5]	Th/U (magma)[6]	^{206}Pb/^{204}Pb[7]	^{206}Pb/^{238}U (±2σ %)[8]	^{207}Pb/^{235}U (±2σ %)[8]	^{207}Pb/^{206}Pb (±2σ %)[8]
01 (13)	1.06	17.0	0.71	23.89	3.212	1281	0.0681 (0.22)	0.5182 (0.54)	0.0552 (0.43)
02 (2)	1.22	34.0	1.30	26.19	3.697	1355	0.0682 (0.17	0.5204 (0.49)	0.0554 (0.40)
03 (3)	0.41	35.0	0.74	47.30	1.242	2956	0.0681 (0.17)	0.5192 (0.29)	0.0553 (0.19)
04 (7)	0.75	14.5	1.36	10.67	2.273	625	0.0681 (0.19)	0.5210 (0.98)	0.0555 (0.87)
05 (12)	0.39	12.6	0.90	14.03	1.182	893	0.0681 (0.19)	0.5204 (0.71)	0.0555 (0.61)
06 (6)	0.75	19.3	0.82	23.47	2.273	1354	0.0693 (0.18)	0.5312 (0.50)	0.0556 (0.40)

[1]Fraction is the CA-ID-TIMS grain number (SIMS grain number). (See Fig. 7a, e, f and g for images of these zircons.)
[2]Thorium contents calculated from radiogenic ^{208}Pb and ^{230}Th-corrected ^{206}Pb/^{238}U date of the sample, assuming concordance between U–Pb and Th–Pb systems.
[3]Total mass of radiogenic Pb.
[4]Total mass of common Pb.
[5]Ratio of radiogenic Pb (including ^{208}Pb) to common Pb.
[6]Th/U ratio of magma from which mineral crystallized.
[7]Measured ratio corrected for fractionation and spike contribution only.
[8]Measured ratios corrected for fractionation, tracer and blank. Uncertainty reported at the ±2σ level in per cent.
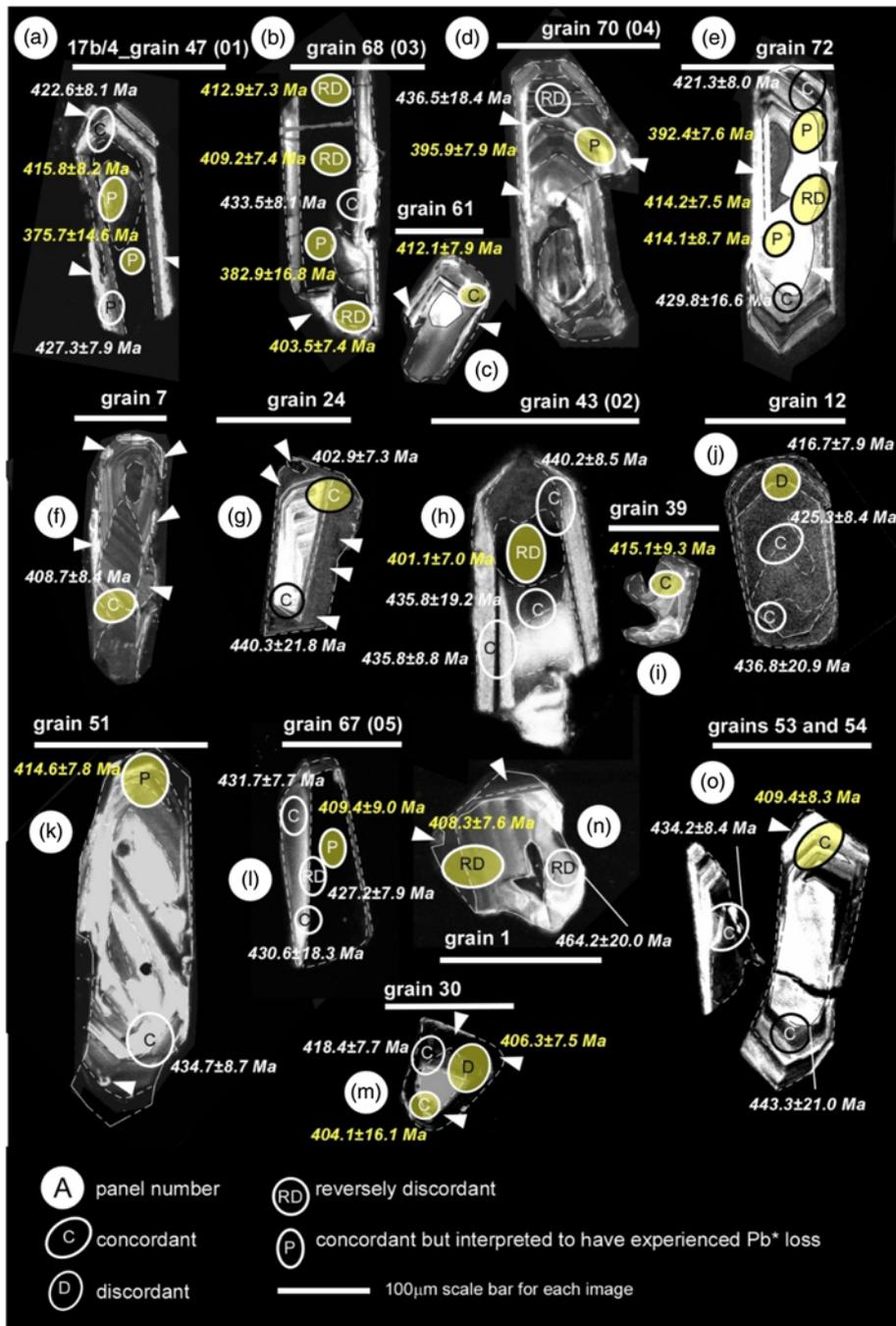
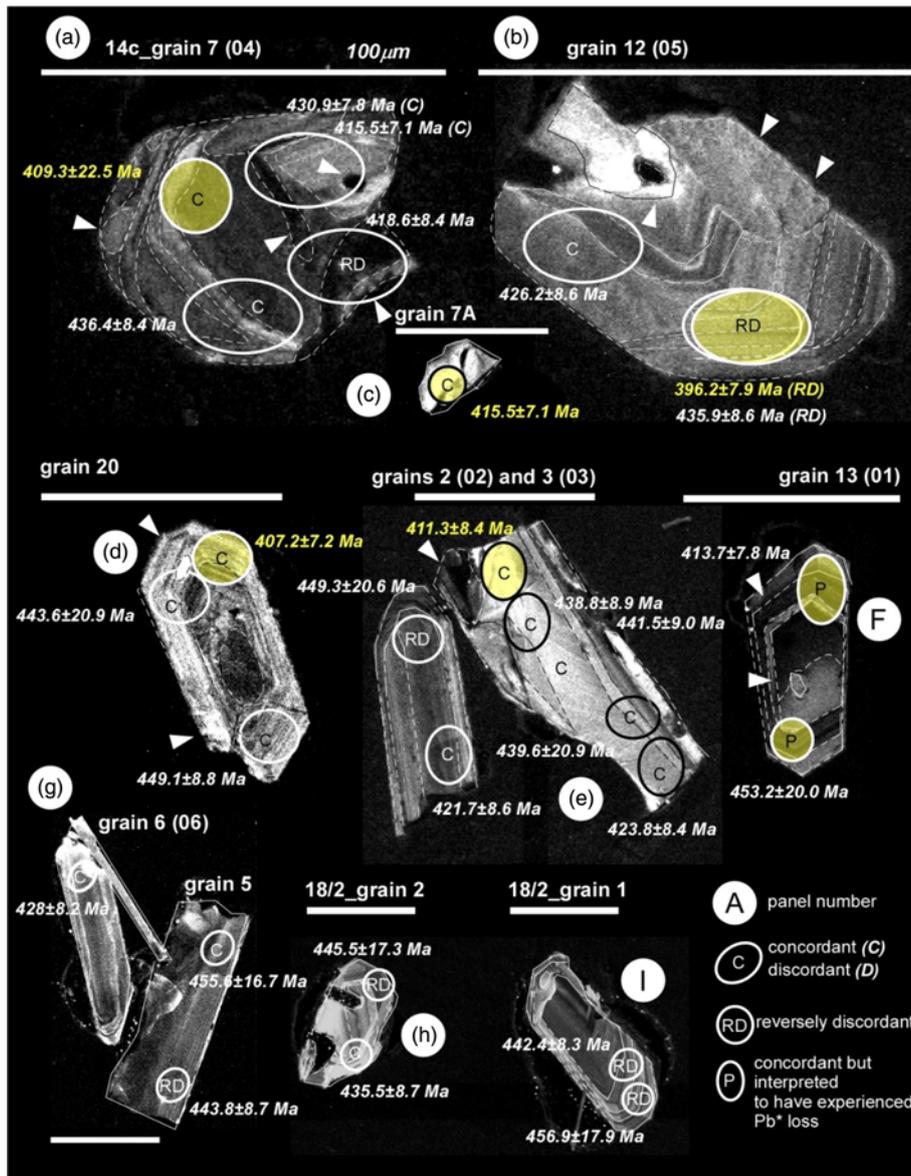**Fig. 6.** (**a–o**) CL images of zircon grains with Přídolí and younger ^{238}U–^{206}Pb SIMS ages in sample 17b/4. Grain numbers are indicated using SIMS zircon number (CA-ID-TIMS sample number, if applicable). The scale bar for each grain represents 100 μm. Yellow spots highlight the youngest ^{238}U–^{206}Pb ages (±1σ). Lines on each grain indicate key zoning features. Abbreviations are explained in the key. (See Table 1 and supplementary data for analytical results.) Arrowheads show features that may have played a role in influencing the SIMS ages.

Ultimately, we are interested in finding what we can argue is the youngest, reliable zircon age for the Ludlow Bone Bed (sample 17b/4) and the Platyschisma Shale (sample 14c) members.

The uncertainty in SIMS ages is more significant than that achieved using CA-ID-TIMS (e.g. Mattinson 2005; Condon and Bowring 2011). However, the complex zonation and broad age distributions indicated by the zircon results and CL images suggest that at first order, an *in situ* (in grain scale) approach like the one we apply is ideal for examining the U–Pb systematics of zircons and their zoning patterns. Following SIMS analysis, CA-ID-TIMS removes areas of Pb loss and metamict zones allowing for high-precision radioisotope U–Pb geochronology.

The CA-ID-TIMS ^{206}Pb/^{238}U ages, 424.91 ± 0.34/0.42/0.63 Ma (sample 17b/4) and 424.85 ± 0.32/0.41/0.62 Ma (sample 14c) (Fig. 5; Tables 3 and 5), are our best estimate of the maximum ages of deposition of the Ludlow Bone Bed and Downton sample, respectively. The Ludlow Bone Bed is thus probably late Silurian

(latest Přídolí) in age. It should be noted that these ages are indistinguishable from the youngest, most concordant SIMS zircon ages from spots we consider to be consistent with crystallization as opposed to alteration (Tables 1 and 2) as well as SIMS ages from the individual grains (Figs 6 and 7). These ages are also indistinguishable from the weighted mean of the concordant SIMS ages (421.7 ± 10.8 Ma for sample 17b/4 and 420.5 ± 21.4 Ma for sample 14c). We note that Brookfield *et al.* (2020) indicated a 420 Ma age for this unit based on the SIMS results. However, the CA-ID-TIMS ages reported here should be considered more precise and used for constraining the timing of maximum deposition.

The CA-ID-TIMS ages we obtain from the Ludlow Bone Bed Member (17b/4) and the Platyschisma Shale Member (14c) are strikingly similar. This observation is consistent with their tidal flat setting and suggestions of rapid sedimentological changes during the closure of the Iapetus Ocean (Allen 1985; Cave and Loydell

Fig. 7. (**a–f**) CL images of zircon grains with Přídolí and younger ^{238}U–^{206}Pb SIMS ages in sample 14c. Grain numbers are indicated using SIMS zircon number (CA-ID-TIMS sample number, if applicable). (**g**) shows grains 5 and 6 from sample 14c; (**h**) and (**i**) are all results from sample 18/2. The scale bar for each grain represents 100 μm. Yellow spots highlight the youngest ^{238}U–^{206}Pb ages (±1σ). Lines on each grain indicate key zoning features. Abbreviations are explained in the key. (See Table 1 and supplementary data for analytical results.) Arrowheads show features that may have played a role in influencing the SIMS ages.

1998). The zircon ^{207}Pb/^{206}Pb age from an ash layer 15 m below the Ludlow Bone Bed from the Upper Whitcliffe Formation is 420.2 ± 3.9 Ma (Tucker 1991; Tucker and McKerrow 1995), and has been recalculated to be 420.88 ± 1.04 Ma (weighted mean ^{238}U–^{206}Pb, Schmitz 2012). Despite being stratigraphically lower than the Ludlow bone beds, this age is younger than the maximum deposition age we calculate. However, the difference may be attributed to the approach applied to date the zircons grains. CA-ID-TIMS ages are from individual zircon grains that have been treated to remove metamict and alteration zones. In contrast, the Upper Whitcliffe Formation age is an average of four concordant zircon dates composed of 5–20 grains, dated using conventional ID-TIMS methods (420.4, 419.4, 422.9 and 418.2 Ma, Tucker 1991). We suggest that the Upper Whitcliffe Formation requires a modern-day zircon dating campaign to obtain an accurate and precise age constraint.

Zircon source

Based on bentonite bed thickness in the field area and the ages of the zircons, the volcanism that produced the zircons dated in this paper probably originated from within the Welsh Basin (Ray 2007). Geochemical evidence from the basin shows a period of late Tremadoc arc volcanism followed by Arenig–Caradoc backarc extension reflected by a transition from a volcanic arc to a marginal basin-type setting (Bevins et al. 1984; Kokelaar 1988; Thorpe et al. 1989; McCann 1991). Both the Midland Platform and Welsh Basin are characterized by bentonite clay-rich beds, which appear to have a subduction-related calc-alkaline, granodiorite source (e.g. Butler 1937; Teale and Spears 1986; Huff et al. 1996; Cave and Loydell 1998; Ray 2007; Ray et al. 2011). Many of its bentonites show evidence of post-depositional compaction and bioturbation, but their thickness suggests less energetic eruptions as opposed to more distal source volcanism. The majority of the volcanism is speculated to have been subaerial (e.g. Bevins 1982), and some deposits were subjected to tectonic movements and mass-gravity flows, and thus record secondary distribution processes (Kokelaar et al. 1984a, b, 1985; Ray 2007; Rogers 2017).

Although volcanism in the vicinity of the field area has been reported to have ended before the late Caradoc (c. 450 Ma, age from Dong et al. 1997; Stillman and Francis 1979; Brenchley et al. 2006), seven zircon grains from bentonite from the West Midlands (Wren's Nest Hill Bentonite 15) have an age of 427.9 ± 0.3 Ma (MSWD = 3.2), interpreted to be the best estimate for the age of the bentonite (Cramer et al. 2012). Three older zircon ages from the sample (428.8 ± 0.4, 429.7 ± 0.4 and 431.1 ± 0.6 Ma) are interpreted to
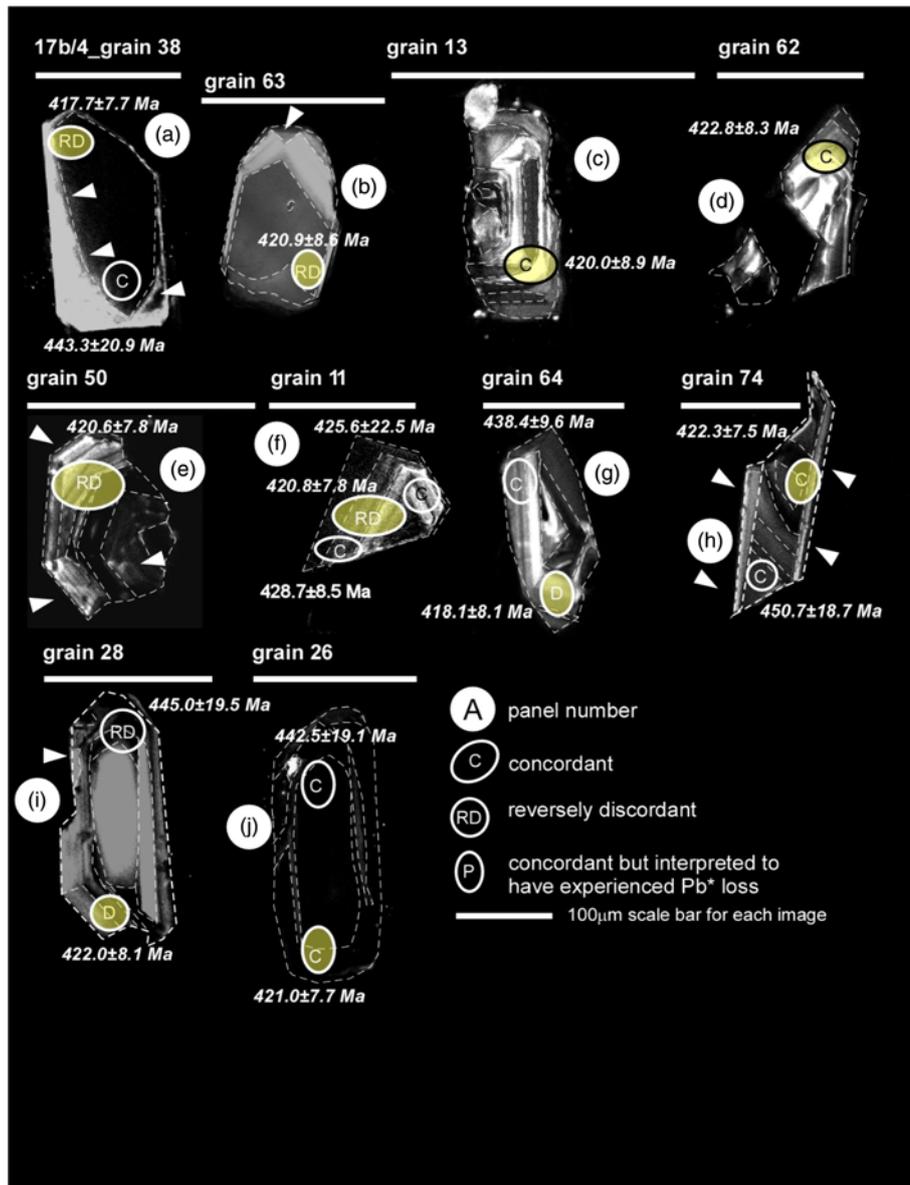
Fig. 8. (**a**–**j**) CL images of zircon grains with Ludlow to Přídolí ^{238}U–^{206}Pb SIMS ages in sample 17b/4. The scale bar for each grain represents 100 μm. Yellow spots highlight the ^{238}U–^{206}Pb ages (±1σ) that are within this range. Lines on each grain indicate key zoning features. Abbreviations are explained in the key. (See Table 1 and supplementary data for analytical results.) Arrowheads show features that may have played a role in influencing the SIMS ages.

reflect xenocrystic material incorporated during magmatic or sedimentary processes. In contrast, one younger result is interpreted to reflect Pb loss (426.9 ± 0.4 Ma). Vitroclastic tuffs and a turbiditic tuffaceous limestone of Wenlock age are also present in the eastern sides of the basin (Cave and Loydell 1998). Rb–Sr ages from the Ashgillian Stockdale Rhyolite in the Lake District yields 421 ± 3 Ma (Gale *et al.* 1979). Overall, the ages we report here are consistent with zircon ages from bentonites located nearby and
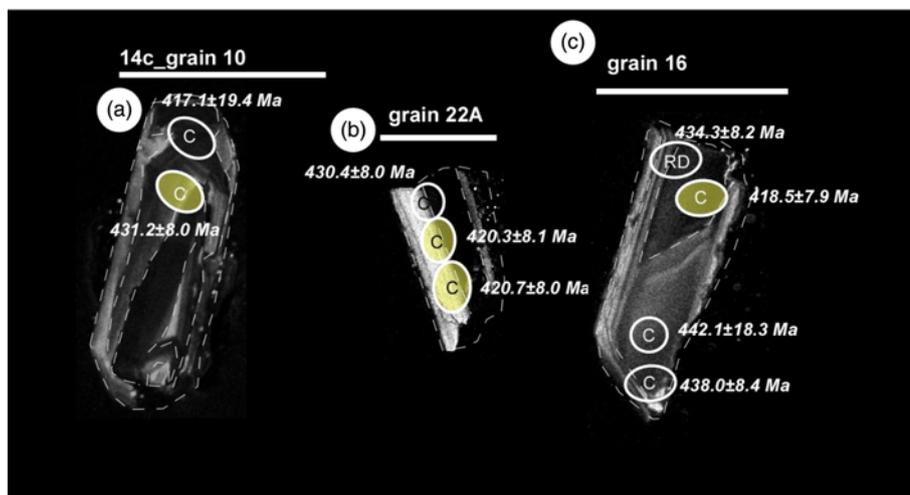
Fig. 9. (**a**–**c**) CL images of zircon grains with Ludlow to Přídolí ^{238}U–^{206}Pb SIMS ages in sample 14c. Other zircons from this sample are shown in Figure 6a and e. Scale bar for each grain represents 100 μm. Yellow spots highlight the ^{238}U–^{206}Pb ages (±1σ) that are within this range. Lines on each grain indicate key zoning features. C, concordant; RD, reversely discordant. (See Table 1 and supplementary data for analytical results.) Arrowheads show features that may have played a role in influencing the SIMS ages.

suggest that volcanic activity is probably a viable source for zircon in these rocks.

Significance of Devonian SIMS U–Pb ages

Concordant Devonian ^{238}U–^{206}Pb SIMS ages average 409.5 ± 8.2 Ma in Ludlow Bone Bed sample 17b/4 and 410.7 ± 5.9 Ma in Platyschisma Shale Member sample 14c. If these are taken as crystallization ages, they could date maximum deposition of the bone beds. We find this scenario less likely, based on the fact that we know of no documented volcanism in the Welsh Basin at this time and the CL images that suggest the ages record the recrystallization of specific zones in the crystals that appear altered as a result of radiation damage. None of the CA-ID-TIMS zircon grains yield these younger ages, even though some of the grains targeted for analyses had Devonian SIMS results.

Radiation damage can occur in natural zircon and affect only zircons that had particular U or Th contents and experienced high amounts of α decay (e.g. Nasdala et al. 2001). Pb can be lost via fast-pathway diffusion from damaged portions of the zircon lattice (Condon and Bowring 2011), resulting in the age distribution we observe. Many natural zircons are often heterogeneously metamict (see review by Nasdala et al. 2001), and this process appears to have affected a number of the 'Devonian' grains reported here. Any zircon grains with younger ages in their core regions compared with those obtained from their rim areas were not considered when assessing the depositional age of the section.

It should be noted that the NW portion of the Welsh Basin experienced low prehnite–pumpellyite-, pumpellyite–actinolite- and greenschist-facies metamorphism (Bevins 1978; Roberts 1981; Bevins 1982; Kokelaar et al. 1984a, b), and this diagenetic to low-grade metamorphism may have begun in the mid- to late Silurian (e.g. 430–400 Ma; Roberts et al. 1996; c. 421 Ma, K–Ar bentonites, Dong et al. 1997, 417 ± 11 Ma U–Pb and 422 ± 24 Ma Pb–Pb of authigenic monazite and apatite, Evans and Zalasiewicz 1996). Fission-track ages from a middle Ludlow bentonite collected c. 2.5 km west of the Ludford Lane and Ludford Corner samples dated in this study are 404 ± 12 and 409 ± 9 Ma and suggest that the unit did not achieve conditions >175°C (Ross et al. 1982; see a critical response to these ages by Gale and Beckinsale 1983). The conodont colour alteration index also supports the thermal conditions, as conodonts from the rocks are pristine and show no evidence of thermal maturation. Fission-track ages from equivalent rocks to these reported elsewhere are younger (398 ± 12 and 389 ± 10 Ma; Ross et al. 1977; Gale et al. 1979). Huff et al. (1996) reported K–Ar ages from illite extracted from Ludlow bentonites that range from 341 ± 6 to 293 ± 6 Ma, and suggested that their depositional age is 410 Ma.

We speculate, primarily on the basis of the CL textures, that the concordant Devonian ages could constrain an episode of zircon recrystallization in situ (in the grain itself). In this scenario, zircon grains that experienced radiation damage within their cores or in specific rim regions recrystallized. The sedimentological disconformity in which the zircons were extracted marks abrupt changes in chemistry from an alkali clay Ca-rich, cationic transfer-type environment (Whitcliffe Formation) to an acid–alkali, anionic, Fe-rich brucite-type–hydrotalcite–hollandite-type transfer environment (e.g. Antia 1980; Allen 1985). This significant, corrosive environment change may have facilitated the dissolution of zircon, whereas the thermal energy needed to anneal could have been driven by widespread tectonic activity as a result of the closure of the Iapetus Ocean (e.g. Butler 1990; also Woodcock 1988; Woodcock and Gibbons 1988; Dewey and Rosenbaum 2008) or via the diagenesis of the sedimentary unit. Some of the zircon grains, which may have already been in a weakened state owing to radiation damage accumulation, experienced an episode of annealing and recrystallization that is recorded by their youngest,

concordant ages. Annealing of the radiation damage generated in α-decay events is a common phenomenon in natural zircons and occurs at igneous (900°C) or metamorphic conditions (600–650°C) in the presence of fluids (Mursic et al. 1992; Mezger and Krogstad 1997; Rizvanova et al. 2000). However, over more extended intervals of geological time, the process can occur at the Earth's surface temperatures (Meldrum et al. 1988; Nasdala et al. 2001). Nasdala et al. (2001) suggested that annealing of damage zones in zircons may occur at conditions of 200–250°C over the geological timescales that would be observed here.

Implications for timing biotic events

The CA-ID-TIMS ages reported in this study overlap the basal Přídolí age (423.0 ± 2.3 Ma) in its stratotype (Požáry Section, Reporyje, Prague, Czech Republic; Holland 1985). Therefore the Ludlow Bone Bed and the base of the local Downton Group can be taken to approximate to the base of the Přídolí Series in the Welsh Borderland rather than the mid-Ludfordian as suggested by Loydell and Fryda (2011). The Ludlow and Downton bone beds are also considered to be contemporaneous at the level of precision obtained by our experiments. The ages obtained are older than those for other land arthropod-bearing sediments in the British Isles, such as the Cowie Harbour Fish Bed and its air-breathing millipede (^{238}U–^{206}Pb laser ablation inductively coupled plasma mass spectrometry (LA-ICP-MS), 414.3 ± 7.1 Ma; Suarez et al. 2017). The absolute age is older than the Rhynie Chert with its more advanced and better preserved terrestrial biota (Trewin 1994) where the hydrothermal activity has been dated at 407.6 ± 2.2 Ma (^{40}Ar/^{39}Ar, systematic uncertainty, Mark et al. 2011, 2013) and an andesite just below the Chert has yielded a TIMS U–Pb zircon age of 411.5 ± 1.3 Ma (late Lochkovian, an average of $n = 4$ grains) (Parry et al. 2011). However, we note that the two youngest zircon ^{238}U–^{206}Pb ages overlap with the ^{40}Ar/^{39}Ar age reported by Mark et al. (2011, 2013).

The CA-ID-TIMS ages obtained here are older than the currently assigned Silurian–Devonian boundary, dated at 419.2 ± 3.2 Ma (Cohen et al. 2020) or 421.3 ± 0.9 Ma (Husson et al. 2016). A volcanic ash 20 m above the Silurian–Devonian biostratigraphic boundary in the Helderberg Limestone of eastern North America (H5-1), gave a youngest ID-TIMS U–Pb concordant zircon age of 417.22 ± 0.21 Ma, whereas one just above the boundary (H2 = 1) has a youngest concordant age of 418.42 ± 0.21 Ma (Husson et al. 2016). Correlative ash to the latter also yielded a youngest concordant U–Pb age of 415.6 ± 1.1 Ma (12-grain fraction analysed) (Tucker et al. 1998).

Many recent calibrations of the geological timescale have relied heavily on statistical techniques in conjunction with best-fit line techniques for estimating numerical ages for chronostratigraphic boundaries. For example, the Silurian timescale is based on calibrating a constrained optimization (CONOP) composite graptolite zonation to selected radioisotopic ages (e.g. Smith et al. 2015). Precise radioistopic dating of ashes (or even detrital zircons) in fossiliferous sections, if available, can assist with the evaluation of these ages. Although the use of in situ approaches, such as SIMS and LA-ICP-MS, is useful for generating large volumes of zircon age data, the precision is too low for constraining boundaries between geological time or evaluating the rate and timing of land colonization by biota. However, these approaches help identify grains that could be re-dated for higher precision results and assist in developing testable hypotheses. The refinement of the youngest zircons using CA-ID-TIMS allows for the removal of ages that should not be considered for assessing deposition and for constraining the timing of critical stratigraphic sections that have recognized importance in identifying significant biotic changes in Earth's history.

Scientific editing by Stephen Daly

References

Agassiz, J.L.R. 1839. Fishes of the Upper Ludlow Rock. *In*: Murchison, R.I. (ed.) *The Silurian System*. John Murray, London, 605–607.

Aldridge, R.J. and Schönlaub, H.-P. 1989. Conodonts. *National Museum of Wales Geological Series*, **9**, 274–279.

Aldridge, R.J. and Smith, M.P. 1985. *Lower Palaeozoic succession of the Welsh Borderland. Fourth European Conodont Symposium (ECOS IV) Field Excursion B, Guidebook*, University of Nottingham, Nottingham, UK.

Allen, J.R.L. 1985. Marine to fresh water: the sedimentology of the interrupted environmental transition (Ludlow–Siegenian) in the Anglo-Welsh region. *Philosophical Transactions of the Royal Society of London, Series B*, **B309**, 85–104.

Antia, D.D.J. 1980. *Palaeontological and Sedimentological Studies on the Upper Silurian Ludlow–Downton Series Transition in the Welsh Borderlands and some Phanerozoic Bone-Beds*. PhD thesis, Glasgow University.

Antia, D.D.J. and Whitaker, J.H.M. 1978. A scanning electron microscope study of the fishes of the Upper Silurian Ludlow bone bed. *In*: Whalley, W.B. (ed.) *Scanning Electron Microscopy in the Study of Sediments*. Elsevier Geo-Abstracts, Norwich, 119–136.

Bassett, M.G. 1985. Towards a common language in stratigraphy. *Episodes*, **8**, 87–92, https://doi.org/10.18814/epiiugs/1985/v8i2/002

Bassett, M.G., Lawson, J.D. and White, D.E. 1982. The Downton Series as the fourth series of the Silurian System. *Lethaia*, **15**, 1–24, https://doi.org/10.1111/j.1502-3931.1982.tb01114.x

Bevins, R. 1978. Pumpellyite-Bearing Basic Igneous Rocks from the Lower Ordovician of North Pembrokeshire, Wales. *Mineralogical Magazine*, **42**, 81–83, https://doi.org/10.1180/minmag.1978.042.321.10

Bevins, R.E. 1982. Petrology and geochemistry of the Fishguard Volcanic Complex, Wales. *Geological Journal*, **17**, 1–21, https://doi.org/10.1002/gj.3350170102

Bevins, R.E., Kokelaar, B.P. and Dunkley, P.N. 1984. Petrology and geochemistry of lower to middle Ordovician igneous rocks in Wales: a volcanic arc to marginal basin transition. *Proceedings of the Geologists' Association*, **95**, 337–347, https://doi.org/10.1016/S0016-7878(84)80064-4

Blain, J.A., Ray, D.C. and Wheeley, J.R. 2016. Carbon isotope ($\delta^{13}C_{carb}$) and facies variability at the Wenlock–Ludlow boundary (Silurian) of the Midland Platform, UK. *Canadian Journal of Earth Sciences*, **53**, 725–730, https://doi.org/10.1139/cjes-2015-0194

Bourgeois, J. 2009. Geologic effects and records of tsunamis. In: Robinson, A.R., Bernard, E.N. (eds) *The Sea*, Vol. 15: *Tsunamis* Harvard University Press, 53–91.

Bowring, J.F., McLean, N.M. and Bowring, S.A. 2011. Engineering cyber infrastructure for U–Pb geochronology: Tripoli and U–Pb_Redux. *Geochemistry, Geophysics, Geosystems*, **12**, Q0AA19, https://doi.org/10.1029/2010GC003479

Brenchley, P.J., Rushton, A.W.A., Howells, M. and Cave, R. 2006. Cambrian and Ordovician: the early Palaeozoic tectonostratigraphic evolution of the Welsh Basin, Midland and Monian Terranes of Eastern Avalonia. *In*: Brenchley, P.W. and Rawson, P.F. (eds) *The Geology of England and Wales*, 2nd edn. Geological Society, London, 25–74, https://doi.org/10.1144/GOEWP.3

Brookfield, M.E. 2004. Deposits of tsunamis and their recognition. *In*: Leroy, S., Ballouche Sabar, M.S.O. and Philip, S. (eds) *Rapid and catastrophic environmental changes in the Holocene and human response. Proceedings of the first joint meeting of IGCP 490 and ICSU Environmental catastrophes in Mauritania, the desert and the coast January 4–18, 2004*, http://at.yorku.ca/c/a/m/u/08.htm

Brookfield, M.E., Schellnutt, G., Qi, L., Hannigan, R., Bhat, M. and Wignall, P.B. 2010. Platinum element group variations at the Permo-Triassic boundary in Kashmir and British Columbia and their significance. *Chemical Geology*, **272**, 12–19, https://doi.org/10.1016/j.chemgeo.2010.01.008

Brookfield, M.E., Catlos, E.J. and Suarez, S.E. 2020. Myriapod divergence times differ between molecular clock and fossil evidence: U/Pb zircon ages of the earliest fossil millipede-bearing sediments and their significance. *Historical Biology*, https://doi.org/10.1080/08912963.2020.1762593

Butler, A.J. 1937. On Silurian and Cambrian rocks encountered in a deep boring at Walsall, South Staffordshire. *Geological Magazine*, **74**, 241–257, https://doi.org/10.1017/S0016756800089822

Butler, J. 1990. A review of the tectonic history of the Shropshire area. *Proceedings of the Shropshire Geological Society*, **9**, 20–34.

Calner, M. 2008. Silurian global events; at the tipping point of climate change. *In*: Elewa, A.M.T. (ed.) *Mass Extinction*. Springer, Berlin, 21–57.

Cave, R. and Loydell, D.K. 1998. Wenlock volcanism in the Welsh Basin. *Geological Journal*, **33**, 107–120, https://doi.org/10.1002/(SICI)1099-1034(1998040)33:2<107::AID-GJ778>3.0.CO;2-R

Chlupác, I. 1972. The Siluro-Devonian Boundary in the Barrandian. *Bulletin of Canadian Petroleum Geology*, **20**, 104–174.

Cohen, K.M., Finney, S.C., Gibbard, P.L. and Fan, J.-X. 2020. The ICS International Chronostratigraphic Chart. *Episodes*, **36**, 199–204, https://stratigraphy.org/icschart/ChronostratChart2020-03.pdf [last accessed 10 August 2020] https://doi.org/10.18814/epiiugs/2013/v36i3/002

Condon, D.J. and Bowring, S.A. 2011. A user's guide to Neoproterozoic geochronology. *Geological Society, London, Memoirs*, **36**, 135–149, https://doi.org/10.1144/M36.9

Condon, D.J., Schoene, B., McLean, N.M., Bowring, S.A. and Parrish, R.R. 2015. Metrology and traceability of U–Pb isotope dilution geochronology (EARTHTIME Tracer Calibration Part I). *Geochimica et Cosmochimica Acta*, **164**, 464–480, https://doi.org/10.1016/j.gca.2015.05.026

Corfu, F. 2013. A century of U–Pb geochronology: The long quest toward concordance. *Geological Society of America Bulletin*, **125**, 33–47, https://doi.org/10.1130/B30698.1

Cramer, B.J., Condon, D.J. *et al.* 2012. U–Pb (zircon) age constraints on the timing and duration of Wenlock (Silurian) paleocommunity collapse and recovery during the "Big Crisis". *Geological Society of America Bulletin*, **124**, 1841–1857, https://doi.org/10.1130/B30642.1

Dewey, J.F. and Rosenbaum, M.S. 2008. Future avenues of research in the Welsh Borderland, with particular reference to terrane tectonics. *Proceedings of the Shropshire Geological Society*, **13**, 104–113.

Dewey, J.F. and Strachan, R.A. 2003. Changing Silurian–Devonian relative plate motion in the Caledonides: sinistral transpression to sinistral transtension. *Journal of the Geological Society, London*, **160**, 219–229, https://doi.org/10.1144/0016-764902-085

Dewey, J.F., Dalziel, I.W.D., Reavy, R.J. and Strachan, R.A. 2015. The Neoproterozoic to Mid-Devonian evolution of Scotland: a review and unresolved issues. *Scottish Journal of Geology*, **51**, 5–30, https://doi.org/10.1144/sjg2014-007

Dineley, D. and Metcalf, S.J. 1999. *Fossil Fishes of Great Britain*. Joint Nature Conservation Committee, Geological Conservation Review Series, **16**.

Dong, H., Hall, C.M., Halliday, A.N., Peacor, D.R., Merriman, R.J. and Roberts, B. 1997. $^{40}Ar/^{39}Ar$ illite dating of Late Caledonian (Acadian) metamorphism and cooling of K-bentonites and slates from the Welsh Basin, UK. *Earth and Planetary Science Letters*, **150**, 337–351, https://doi.org/10.1016/S0012-821X(97)00100-3

Dunlop, J.A. 1996. A trigonotarbid arachnid from the Upper Silurian of Shropshire. *Palaeontology*, **39**, 605–614.

Edwards, D. 1996. New insights into early land ecosystems: A glimpse of a Lilliputian world. *Reviews in Palaeobotany and Palynology*, **90**, 159–174, https://doi.org/10.1016/0034-6667(95)00081-X

Edwards, D. and Kenrick, P. 2015. The early evolution of land plants, from fossils to genomics: a commentary on Lang (1937) 'On the plant-remains from the Downtonian of England and Wales'. *Philosophical Transactions of the Royal*

Zircon ages from the Ludlow and Downton bone beds

Society of London, Part B, **370**, 20140343, https://doi.org/10.1098/rstb.2014.0343

Evans, J. and Zalasiewicz, J. 1996. U–Pb, Pb–Pb and Sm–Nd dating of authigenic monazite: implications for the diagenetic evolution of the Welsh Basin. *Earth and Planetary Science Letters*, **144**, 421–433, https://doi.org/10.1016/S0012-821X(96)00177-X

Gale, N. and Beckinsale, R. 1983. Comments on the paper 'Fission-track dating of British Ordovician and Silurian stratotypes' by R. J. Ross and others. *Geological Magazine*, **120**, 295–302, https://doi.org/10.1017/S0016756800025486

Gale, N.H., Beckinsale, R.D. and Wadge, A.J. 1979. A Rb/Sr whole rock isochron for the Stockdale Rhyolite of the English Lake District and a revised mid-Palaeozoic time-scale. *Journal of the Geological Society, London*, **136**, 235–242, https://doi.org/10.1144/gsjgs.136.2.0235

Gehrels, G. 2012. Detrital zircon U–Pb geochronology: current methods and new opportunities. *In*: Busby, C. and Azor, A. (eds) *Tectonics of Sedimentary Basins: Recent Advances*, 1st edn. Blackwell, Oxford, 47–62.

Guillong, M., von Quadt, A., Sakata, S., Peytcheva, I. and Bachmann, O. 2014. LA-ICP-MS Pb–U dating of young zircons from the Kos–Nisyros volcanic centre, SE Aegean arc. *Journal of Analytical and Atomic Spectrometry*, **29**, 863–970, https://doi.org/10.1039/C4JA00009A

Hanchar, J.M. and Miller, C.F. 1993. Zircon zonation patterns as revealed by cathodoluminescence and backscattered electron images: Implications for interpretation of complex crustal histories. *Chemical Geology*, **110**, 1–13, https://doi.org/10.1016/0009-2541(93)90244-D

Harley, J. 1861. On the Ludlow Bone Bed and its crustacean remains. *Quarterly Journal of the Geological Society of London*, **17**, 542–552, https://doi.org/10.1144/GSL.JGS.1861.017.01-02.47

Hauser, L. 2019. *The upper Silurian Downton Bone Bed of Weir Quarry, Herefordshire, England*. PhD thesis, University of Portsmouth.

Hinde, G.J. 1904. The Bone-bed in the Upper Ludlow formation. *Proceedings of the Geologists' Association*, **18**, 443–446, https://doi.org/10.1016/S0016-7878(04)80047-6

Hoke, G.D., Schmitz, M.D. and Bowring, S.A. 2014. An ultrasonic method for isolating nonclay components from clay-rich material. *Geochemistry, Geophysics, Geosystems*, **15**, 492–498, https://doi.org/10.1002/2013GC005125

Holland, C.H. 1982. The state of Silurian stratigraphy. *Episodes*, **3**, 21–23, https://doi.org/10.18814/epiiugs/1982/v5i3/004

Holland, C.H. 1985. Series and stages of the Silurian system. *Episodes*, **2**, 101–103, https://doi.org/10.18814/epiiugs/1985/v8i2/005

Holland, C.H., Lawson, J.D. and Walmsley, V.D. 1963. The Silurian rocks of the Ludlow district, Shropshire. *Bulletin of the British Museum (Natural History) Geology Series*, **8**, 95–171.

Horstwood, M.S., Košler, J. *et al.* 2016. Community-Derived Standards for LA-ICP-MS U–(Th–)Pb Geochronology – Uncertainty Propagation, Age Interpretation and Data Reporting. *Geostandards and Geoanalytical Research*, **40**, 311–332, https://doi.org/10.1111/j.1751-908X.2016.00379.x

Huff, W.D., Morgan, D.J. and Rundle, C.C. 1996. Silurian K-bentonites of the Welsh Borderlands: Geochemistry, mineralogy and K–Ar ages of illitization. British Geological Survey, WG/96/045 (unpublished), http://nora.nerc.ac.uk/id/eprint/7090/1/WG96045.pdf

Husson, J.M., Schoene, B., Bluher, S. and Maloof, A.C. 2016. Chemostratigraphic and U–Pb geochronologic constraints on carbon cycling across the Silurian–Devonian boundary. *Earth and Planetary Science Letters*, **436**, 108–120, https://doi.org/10.1016/j.epsl.2015.11.044

Huyskens, M.H., Tsuyoshi Iizuka, T. and Amelin, Y. 2012. Evaluation of colloidal silicagels for lead isotopic measurements using thermal ionisation mass spectrometry, *Journal of Analytical Atomic Spectrometry*, **27**, 1439–1446, https://doi.org/10.1039/c2ja30083d

Jaffey, A.H., Flynn, K.F., Glendenin, L.E., Bentley, W.C. and Essling, A.M. 1971. Precision measurement of half-lives and specific activities of ^{235}U and ^{238}U. *Physics Reviews*, **C4**, 1889–1906, https://doi.org/10.1103/PhysRevC.4.1889

Jeram, A.J., Selden, P.A. and Edwards, D. 1990. Land animals in the Silurian: arachnids and myriapods from Shropshire, England. *Science*, **250**, 658–666, https://doi.org/10.1126/science.250.4981.658

Jones, O.T. 1955. The geological evolution of Wales and the adjacent regions. *Quarterly Journal of the Geological Society of London*, **111**, 323–351, https://doi.org/10.1144/GSL.JGS.1955.111.01-04.17

Keller, C.B., Schoene, B., Barboni, M., Samperton, K.M. and Husson, J.M. 2015. Volcanic–plutonic parity and the differentiation of the continental crust. *Nature*, **523**, 301–307, https://doi.org/10.1038/nature14584

Kokelaar, P. 1988. Tectonic controls of Ordovician arc and marginal basin volcanism in Wales. *Journal of the Geological Society, London*, **145**, 759–775, https://doi.org/10.1144/gsjgs.145.5.0759

Kokelaar, B.P., Howells, M.F., Bevins, R.E. and Roach, R.A. 1984a. Volcanic and associated sedimentary and tectonic processes in the Ordovician marginal basin of Wales: a field guide. *Geological Society, London Special Publications*, **16**, 291–322, https://doi.org/10.1144/GSL.SP.1984.016.01.23

Kokelaar, B.P., Howells, M.F., Bevins, R.E., Roach, R.A. and Dunkley, P.N. 1984b. The Ordovician marginal basin of Wales. *Geological Society, London, Special Publications*, **16**, 245–269, https://doi.org/10.1144/GSL.SP.1984.016.01.19

Kokelaar, B.P., Bevins, R.E. and Roach, R.A. 1985. Submarine silicic volcanism and associated sedimentary and tectonic processes, Ramsey Island, SW Wales.

Journal of the Geological Society, London, **142**, 591–613, https://doi.org/10.1144/gsjgs.142.4.0591

Kříž, J., Jaeger, H., Paris, F. and Schönlaub, H.-P. 1986. Prídolí – the fourth subdivision of the Silurian System. *Jahrbuch der Geologischen Bundesanstalt*, **129**, 291–360.

Krogh, T.E. 1973. A low-contamination method for hydrothermal decomposition of zircon and extraction of U and Pb for isotopic age determinations. *Geochimica et Cosmochimica Acta*, **37**, 485–494, https://doi.org/10.1016/0016-7037(73)90213-5

Lawson, J.D. and White, D.E. 1989. The Ludlow Series in the Ludlow area. *National Museum of Wales Geological Series*, **9**, 73–90.

Loydell, D.K. and Fryda, J. 2011. At what stratigraphical level is the mid Ludfordian (Ludlow, Silurian) positive carbon isotope excursion in the type Ludlow area, Shropshire, England? *Bulletin of Geosciences*, **86**, 197–208, https://doi.org/10.3140/bull.geosci.1257

Lukács, R., Guillong, M., Schmitt, A.K., Molnár, K., Bachmann, O. and Harangi, S. 2018. LA-ICP-MS and SIMS U–Pb and U–Th zircon geochronological data of Late Pleistocene lava domes of the Ciomadul Volcanic Dome Complex (Eastern Carpathians). *Data in Brief*, **18**, 808–813, https://doi.org/10.1016/j.dib.2018.03.100

Manning, P.L. 1993. *Palaeoecology of eurypterids of the Welsh Borderland*. MSc thesis, University of Manchester.

Manning, P.L. and Dunlop, J.A. 1995. The respiratory organs of eurypterids. *Palaeontology*, **38**, 287–297.

Mariano, A.N. 1989. Cathodoluminescence emission spectra of rare earth element activators in minerals. *Mineralogical Society of America and Geochemical Society, Reviews in Mineralogy and Geochemistry*, **21**, 339–348.

Mark, D.F., Rice, C.M., Fallick, A.E., Trewin, N.H., Lee, M.R., Boyce, A. and Lee, J.K.W. 2011. ^{40}Ar/^{39}Ar dating of hydrothermal activity, biota and gold mineralization in the Rhynie hot-spring system, Aberdeenshire, Scotland. *Geochimica et Cosmochimica Acta*, **75**, 555–569, https://doi.org/10.1016/j.gca.2010.10.014

Mark, D.F., Rice, C.M. and Trewin, N.H. 2013. Discussion on 'A high-precision U–Pb age constraint on the Rhynie Chert Konservat-Lagerstätte: time scale and other implications' Journal, Vol. 168, 863–872. *Journal of the Geological Society, London*, **170**, 701–703, https://doi.org/10.1144/jgs2011-110

Märss, T. and Miller, C.G. 2004. Thelodonts and distribution of associated conodonts from the Llandovery–lowermost Lochkovian of the Welsh Borderland. *Palaeontology*, **47**, 1211–1265, https://doi.org/10.1111/j.0031-0239.2004.00409.x

Mattinson, J.M. 2005. Zircon U–Pb chemical abrasion ('CA-TIMS') method: combined annealing and multi-step partial dissolution analysis for improved precision and accuracy of zircon ages. *Chemical Geology*, **220**, 47–66, https://doi.org/10.1016/j.chemgeo.2005.03.011

McCann, T. 1991. Petrological and geochemical determination of provenance in the southern Welsh Basin. *Geological Society, London, Special Publications*, **57**, 215–230, https://doi.org/10.1144/GSL.SP.1991.057.01.17

McLean, N.M., Bowring, J.F. and Bowring, S.A. 2011. An algorithm for U–Pb isotope dilution data reduction and uncertainty propagation. *Geochemistry, Geophysics, Geosystems*, **12**, Q0AA18, https://doi.org/10.1029/2010GC003478

Meldrum, A., Boatner, L.A., Weber, W.J. and Ewing, R.C. 1988. Radiation damage in zircon and monazite. *Geochimica et Cosmochimica Acta*, **62**, 2509–2520, https://doi.org/10.1016/S0016-7037(98)00174-4

Mezger, K. and Krogstad, E.J. 1997. Interpretation of discordant U–Pb zircon ages: An evaluation. *Journal of Metamorphic Geology*, **15**, 127–140, https://doi.org/10.1111/j.1525-1314.1997.00008.x

Miller, C.G. 1995. Ostracode and conodont distribution across the Ludlow/Prídoli boundary of Wales and the Welsh borderland. *Palaeontology*, **38**, 341–384.

Miller, C.G. and Aldridge, R.J. 1993. The taxonomy and apparatus structure of the Silurian distomodontid conodont *Coryssognathus*. *Journal of Micropalaeontology*, **12**, 241–255, https://doi.org/10.1144/jm.12.2.241

Miller, C.G. and Aldridge, R.J. 1997. *Ozarkodina remscheidensis* plexus conodonts from the upper Ludlow (Silurian) of the Welsh Borderland and Wales. *Journal of Micropalaeontology*, **16**, 41–49, https://doi.org/10.1144/jm.16.1.41

Munnecke, A., Calner, M., Harper, D.A.T. and Servais, T. 2010. Ordovician and Silurian sea-water chemistry, sea level, and climate: A synopsis. *Palaeogeography, Palaeoclimatology, Palaeoecology*, **296**, 389–413, https://doi.org/10.1016/j.palaeo.2010.08.001

Murchison, R.I. 1853. On some of the remains of the bone-bed in the Upper Ludlow rocks. *Quarterly Journal of the Geological Society of London*, **9**, 16–17, https://doi.org/10.1144/GSL.JGS.1853.009.01-02.09

Mursic, Z., Vogt, T., Boysen, H. and Frey, F. 1992. Single-crystal neutron diffraction study of metamict zircon up to 2000 K. *Journal of Applied Crystallography*, **25**, 519–523, https://doi.org/10.1107/S0021889892002577

Nasdala, L., Wenzel, M., Vavra, G., Irmer, G., Wenzel, T. and Kober, B. 2001. Metamictisation of natural zircon: accumulation versus thermal annealing of radioactivity-induced damage. *Contributions to Mineralogy and Petrology*, **141**, 125–144, https://doi.org/10.1007/s004100000235

Ogg, J.G., Ogg, G. and Gradstein, F.M. 2008. *Silurian Period. The Concise Geologic Time Scale*. Cambridge University Press, New York, 57–63.

Parrish, R.R. and Krogh, T.E. 1987. Synthesis and purification of ^{205}Pb for U–Pb geochronology. *Chemical Geology*, **66**, 103–110.

Parry, S.F., Noble, S.R., Crowley, Q.J. and Wellman, C.H. 2011. A high-precision U/Pb age constraint on the Rhynie Chert Konservat-Lagerstätten: time scale and other implications. *Journal of the Geological Society, London*, **168**, 863–872, https://doi.org/10.1144/0016-76492010-043

Ray, D., Collings, A., Worton, G. and Jones, G. 2011. Upper Wenlock bentonites from Wren's Nest Hill, Dudley: Comparisons with prominent bentonites along Wenlock Edge, Shropshire, England. *Geological Magazine*, **148**, 670–681, https://doi.org/10.1017/S0016756811000288

Ray, D.C. 2007. The correlation of Lower Wenlock Series (Silurian) bentonites from the Lower Hill Farm and Eastnor Park boreholes, Midland Platform, England. *Proceedings of the Geologists' Association*, **118**, 175–185, https://doi.org/10.1016/S0016-7878(07)80034-4

Remond, G., Cesbron, F., Chapoulie, R., Ohnenstetter, D., Roques-Carmes, C. and Schvoerer, M. 1992. Cathodoluminescence applied to the microcharacterization of mineral materials: a present status in experimentation and interpretation. *Scanning Microscopy*, **6**, 23–68.

Richardson, J.B. and Lister, T.R. 1969. Upper Silurian and lower Devonian spore assemblages from the Welsh borderland and south Wales. *Palaeontology*, **12**, 201–245.

Richardson, J.B. and Rasul, S.M. 1990. Palynofacies in a Late Silurian regressive sequence in the Welsh Borderland and Wales. *Journal of the Geological Society, London*, **147**, 675–686, https://doi.org/10.1144/gsjgs.147.4.0675

Rizvanova, N.G., Levchenkov, O.A., *et al.* 2000. Zircon reaction and stability of the U-Pb isotope system during interaction with carbonate fluid: experimental hydrothermal study. *Contributions to Mineralogy and Petrology*, **139**, 101–114, https://doi.org/10.1007/s004100050576

Roberts, B. 1981. Low grade and very low grade regional metabasic Ordovician rocks of Llŷn and Snowdonia, Gwynedd, North Wales. *Geological Magazine*, **118**, 189–200, https://doi.org/10.1017/S0016756800034385

Roberts, B., Merriman, R.J., Hirons, S.R., Fletcher, C.J.N. and Wilson, D. 1996. Synchronous very low-grade metamorphism, contraction and inversion in the central part of the Welsh Lower Palaeozoic Basin. *Journal of the Geological Society, London*, **153**, 277–285, https://doi.org/10.1144/gsjgs.153.2.0277

Rogers, S. 2017. The occurrence of seismites in the Upper Silurian Whitcliffe Formation of the old Whitcliffe quarry, Ludlow. *Proceedings of the Shropshire Geological Society*, **18**, 61–73.

Ross, R., Naeser, C. *et al.* 1982. Fission-track dating of British Ordovician and Silurian stratotypes. *Geological Magazine*, **119**, 135–153, https://doi.org/10.1017/S0016756800025838

Ross, R.J., Naeser, C.W. *et al.* 1977. Fission-track dating of Lower Paleozoic bentonites in British stratotypes. *3rd International Symposium on the Ordovician System Program Abstracts, Columbus, Ohio*, 4.

Rowlands, M. 1988. Ludford Lane and Ludford Corner; the Ludlow bone bed. *Fossil Forum Magazine*, **2**, 91–100.

Rubatto, D. and Gebauer, D. 2000. Use of cathodoluminescence for U-Pb zircon dating by ion microprobe: Some examples from the Western Alps. *In*: Pagel, M., Barbin, V., Blanc, P. and Ohnenstetter, D. (eds) *Cathodoluminescence in Geosciences*. Springer, Berlin, 373–400.

Rubatto, D. and Hermann, J. 2007. Experimental zircon/melt and zircon/garnet trace element partitioning and implications for the geochronology of crustal rocks. *Chemical Geology*, **241**, 38–61, https://doi.org/10.1016/j.chemgeo.2007.01.027

Schaltegger, U., Schmitt, A. and Horstwood, M.S.A. 2015. U-Th-Pb zircon geochronology by ID-TIMS, SIMS, and laser ablation ICP-MS: recipes, interpretations, and opportunities. *Chemical Geology*, **402**, 89–110, https://doi.org/10.1016/j.chemgeo.2015.02.028

Schmitz, B. 1992. An iridium anomaly in the Ludlow Bone Bed from the Upper Silurian, England. *Geological Magazine*, **129**, 359–362, https://doi.org/10.1017/S0016756800019294

Schmitz, M.D. 2012. Appendix 2 – Radiometric ages used in GTS2012. *In*: Gradstein, F.M., Ogg, J.G., Schmitz, M.D. and Ogg, G.M. (eds) *The Geologic Time Scale*. Elsevier, Amsterdam, 1045–1082, https://doi.org/10.1016/B978-0-444-59425-9.15002-4

Schmitz, M.D., Bowring, S.A. and Ireland, T.R. 2003. Evaluation of Duluth Complex anorthositic series (AS3) zircon as a U-Pb geochronological standard: new high-precision isotope dilution thermal ionization mass spectrometry results. *Geochimica et Cosmochimica Acta*, **67**, 3665–3672, https://doi.org/10.1016/S0016-7037(03)00200-X

Schoene, B., Crowley, J.L., Condon, D.C., Schmitz, M.D. and Bowring, S.A. 2006. Reassessing the uranium decay constants for geochronology using ID-TIMS U-Pb data. *Geochimica et Cosmochimica Acta*, **70**, 426–445, https://doi.org/10.1016/j.gca.2005.09.007

Schönlaub, H.-P. 1986. Conodonts. *Jahrbuch der Geologischen Bundesanstalt*, **129**, 334–337.

Shear, W.A. and Selden, P.A. 1995. Eoarthropleura from the Silurian of Britain and the Devonian of North America. *Neues Jahrbuch für Geologie und Paläontologie, Abhandlungen*, **196**, 347–375.

Shear, W.A., Jeram, A.J. and Selden, P.A. 1998. Centipede legs (Arthropoda, Chilopoda, Scutigeromorpha) from the Silurian and Devonian of Britain and the Devonian of North America. *American Museum Novitates*, **3231**, 1–16.

Siveter, D.J. 2000. The Ludlow Series. *Geological Conservation Review Series*, **19**, 325–425.

Siveter, D.J., Owens, R.M. and Thomas, A.T. 1989. *Silurian field excursions: A geotraverse across Wales and the Welsh Borderland*. National Museum of Wales Geological Series, **10**.

Sláma, J., Košler, J. *et al.* 2008. Plešovice zircon – A new natural reference material for U–Pb and Hf isotopic microanalysis. *Chemical Geology*, **249**, 1–35, https://doi.org/10.1016/j.chemgeo.2007.11.005

Smith, R.D.A. and Ainsworth, R.B. 1989. Hummocky cross-stratification in the Downton of the Welsh borderland. *Journal of the Geological Society, London*, **146**, 897–900, https://doi.org/10.1144/gsjgs.146.6.0897

Smith, A.G., Barry, T. *et al.* 2015. GSSPs, global stratigraphy and correlation. *Geological Society, London, Special Publications*, **404**, 37–67, https://doi.org/10.1144/SP404.8

Spencer, C.J., Kirkland, C.L. and Taylor, R.J.M. 2016. Strategies towards statistically robust interpretations of *in situ* U–Pb zircon geochronology. *Geoscience Frontiers*, **7**, 581–589, https://doi.org/10.1016/j.gsf.2015.11.006

Stacey, J.S. and Kramers, J.D. 1975. Approximation of terrestrial lead isotope evolution by a 2-stage model. *Earth and Planetary Science Letters*, **26**, 207–221, https://doi.org/10.1016/0012-821X(75)90088-6

Steiger, R.H. and Jäger, E. 1977. Subcommission on geochronology: Convention on the use of decay constants in geo- and cosmochronology. *Earth and Planetary Science Letters*, **36**, 359–362, https://doi.org/10.1016/0012-821X(77)90060-7

Stillman, C.J. and Francis, E.H. 1979. Caledonide volcanism in Britain and Ireland. *Geological Society, London, Special Publications*, **8**, 555–577, https://doi.org/10.1144/GSL.SP.1979.008.01.67

Suarez, S.E., Brookfield, M.E., Catlos, E.J. and Stöckli, D.F. 2017. A U–Pb zircon age constraint on the oldest-recorded air-breathing land animal. *PLoS One*, **12**, e0179262, https://doi.org/10.1371/journal.pone.0179262

Symonds, W.S. 1872. *Records of the rocks; or, notes on the geology, natural history, and antiquities of north and south Wales, Devon, and Cornwall*. John Murray, London, https://archive.org/details/recordsofrocksor00symoiala

Teale, T.C. and Spears, A.D. 1986. The mineralogy and origin of some Silurian bentonites, Welsh Borderlands, UK. *Sedimentology*, **33**, 757–765, https://doi.org/10.1111/j.1365-3091.1986.tb01974.x

Thorpe, R.S., Leat, P.T., Bevins, R.E. and Hughes, D.J. 1989. Late-orogenic alkaline/subalkaline Silurian volcanism of the Skomer Volcanic Group in the Caledonides of south Wales. *Journal of the Geological Society, London*, **146**, 125–132, https://doi.org/10.1144/gsjgs.146.1.0125

Trewin, N.H. 1994. Depositional environment and preservation of biota in the Lower Devonian hot-springs of Rhynie, Aberdeenshire, Scotland. *Earth and Environmental Science Transactions of The Royal Society of Edinburgh*, **84**, 433–442, https://doi.org/10.1017/S0263593300006234

Tucker, R.D. 1991. Ordovician and Silurian stratotypes of Britain. *US Geological Survey, Open-File Report*, **91-565**, 57–58.

Tucker, R.D. and McKerrow, W.S. 1995. Early Paleozoic chronology: a review in light of new U–Pb zircon ages from Newfoundland and Britain. *Canadian Journal of Earth Sciences*, **32**, 368–379, https://doi.org/10.1139/e95-032

Tucker, R.D., Bradley, D.C., Ver Straeten, C.A., Harris, A.G., Ebert, J.R. and McCutcheon, S.R. 1998. New U–Pb zircon ages and the duration and division of Devonian time. *Earth and Planetary Science Letters*, **158**, 175–186, https://doi.org/10.1016/S0012-821X(98)00050-8

Turner, S. 1973. Siluro-Devonian thelodonts from the Welsh Borderland. *Quarterly Journal of the Geological Society of London*, **129**, 557–584, https://doi.org/10.1144/gsjgs.129.6.0557

Turner, S. 2000. New Llandovery to early Prídolí microvertebrates including Lower Silurian zone fossil, *Loganellia avonia* nov. sp., from Britain. *Courier Forschungsinstitut Senckenberg*, **223**, 91–127.

Viira, V. and Aldridge, R.J. 1998. Upper Wenlock to lower Pridoli (Silurian) conodont biostratigraphy of Saaremaa, Estonia and a correlation with Britain. *Journal of Micropalaeontology*, **17**, 33–50, https://doi.org/10.1144/jm.17.1.33

Wendt, I. and Carl, C. 1991. The statistical distribution of the mean squared weighted deviation. *Chemical Geology*, **86**, 275–285, https://doi.org/10.1016/0168-9622(91)90010-T

Whitaker, J.H.M. 1962. The geology of the area around Leintwardine, Herefordshire. *Quarterly Journal of the Geological Society of London*, **118**, 319–351, https://doi.org/10.1144/gsjgs.118.1.0319

White, E.I. 1950. The vertebrate faunas of the lower Old Red Sandstone of the Welsh borders. *Bulletin of the British Museum*, **1**, 51–67.

Wiedenbeck, M., Allé, P. *et al.* 1995. Three natural zircon standards for U–Th–Pb, Lu–Hf, trace element and REE analyses. *Geostandards Newsletter*, **19**, 1–23, https://doi.org/10.1111/j.1751-908X.1995.tb00147.x

Wiedenbeck, M., Hanchar, J.M., *et al.* 2004. Further characterisation of the 91500 zircon crystal. *Geostandards and Geoanalytical Research*, **28**, 9–39, https://doi.org/10.1111/j.1751-908X.2004.tb01041.x

Woodcock, N.H. 1988. Strike-slip faulting along the Church Stretton Lineament, Old Radnor Inlier, Wales. *Journal of the Geological Society, London*, **145**, 925–933, https://doi.org/10.1144/gsjgs.145.6.0925

Woodcock, N.H. and Gibbons, W. 1988. Is the Welsh Borderland Fault System a terrane boundary? *Journal of the Geological Society, London*, **145**, 915–923, https://doi.org/10.1144/gsjgs.145.6.0915